

UNITED STATES DEPARTMENT OF THE INTERIOR
GEOLOGICAL SURVEY

THE STRATIGRAPHY AND PHOSPHORITIC ROCKS OF
THE ROBINSON CANYON-LAURELES GRADE AREA
MONTEREY COUNTY, CALIFORNIA

By

Gary A. Younse

Open-file Report
80-318

This report is preliminary and
has not been edited or reviewed
for conformity with Geological
Survey standards of nomenclature

ACKNOWLEDGEMENTS

I would like to thank numerous people who have made this study possible. Calvin H. Stevens of San Jose State University was my major advisor for this thesis. Albert E. Roberts of the U.S. Geological Survey in Menlo Park, Robert E. Garrison of U. C. Santa Cruz, and Marshall Maddock of San Jose State University technically reviewed this thesis. Several other U.S. Geological Survey employees in Menlo Park, California, gave invaluable services. Kristin A. Mcdougall identified the benthonic foraminifers and provided helpful discussion on microfossil significance; Sean M. Stone provided technical assistance in the preparation of microfossil samples; Warren O. Addicott aided in, and confirmed many of the invertebrate megafossil identifications and provided helpful discussions; Charles A. Repenning identified vertebrate megafossil samples; Virgil A. Frizell, Jr. and John C. Tinsley, III supplied aerial photographs; Earl E. Brabb supplied well-log data; Kenneth S. Muir supplied groundwater and geological data; Meade B. Norman and James L. Drinkwater provided technical assistance in X-ray analysis work; Frances R. Mills provided technical assistance and the use of drafting materials; Robert Gulbrandsen supplied chemicals and provided helpful discussions of phosphates; J. L. Harris and L. Mei of the U.S. Geological Survey in Reston, Virginia, and Chris Heropoulos and Leticia

Castilla of the Menlo Park facilities performed semiquantitative chemical analyses on phosphoritic samples; Robert Oscarson provided technical assistance on the scanning electron microscope; and Johnnie M. Denman typed this manuscript.

Special thanks also are due the main property owners of Carmel Valley who made my field investigations possible: Mrs. Jane Dunaway of the Dunaway Ranch; Mr. Kaye Chandler of the Carmel Valley Ranch; Mr. Bill Luttrell, manager of the Rancho San Carlos; and Dr. Jack Stein and Mr. Robert Talbout, co-owners of an undeveloped land parcel.

TABLE OF CONTENTS

	Page
ABSTRACT.....	xii
INTRODUCTION.....	1
Purpose of Investigation.....	1
Previous Studies.....	1
Location and Accessibility.....	2
Geography.....	2
METHODS OF STUDY.....	5
Preliminary Investigation.....	5
Fieldwork.....	5
STRATIGRAPHY.....	7
Basement.....	7
Chamisal Formation.....	10
Robinson Canyon Member.....	11
Distribution and Thickness.....	11
Lithology.....	12
Age and Correlation.....	14
Depositional Environment.....	14
Los Tularcitos Member.....	17
Distribution and Thickness.....	17
Lithology.....	18
Age and Correlation.....	21
Depositional Environment.....	22
Monterey Formation.....	24

	Page
Laureles Sandstone Member.....	26
Distribution and Thickness.....	26
Lithology.....	28
Age and Correlation.....	29
Depositional Environment.....	30
Sandholdt Member.....	31
Distribution and Thickness.....	31
Lithology.....	34
Age and Correlation.....	39
Depositional Environment.....	41
Hames Member.....	43
Distribution and Thickness.....	43
Lithology.....	43
Age and Correlation.....	47
Depositional Environment.....	47
Miscellaneous Surficial Deposits.....	48
TECTONICS AND STRUCTURAL EVOLUTION.....	50
PHOSPHORITIC ROCKS.....	53
Nomenclature.....	53
Stratigraphic Occurrence and Bedding	
Characteristics.....	54
Petrography.....	60
Oolites.....	60
Pellets.....	67

	Page
Non-centered Pellets.....	72
Intraclasts.....	73
Bioclatss.....	76
Geochemistry.....	76
X-ray Analysis.....	80
Scanning Electron Microscopy.....	83
Origins of Phosphoritic Rocks and Conclusions.....	85
REFERENCES CITED.....	100
APPENDICES.....	108
Laboratory Work and Procedures.....	108
Test Well Data.....	110
Paleobathymetry Determined from Foraminifers.....	111
Measured Sections.....	112
Section 8.....	112
Section 60.....	114
Section 109.....	117
Section 191.....	118
Section 259.....	121
Section 276.....	122
Section 332.....	123
Section 399.....	125
Section 467.....	126

LIST OF ILLUSTRATIONS

Figure	Page
1. Location of the Robinson Canyon-Laureles Grade area.....	3
2. Generalized stratigraphic column of the Robinson Canyon-Laureles Grade area.....	8
3. Burrow structures in the basal portion of the Los Tularcitos Member at locality M-Y-471 (plate 3).....	19
4. Sedimentation scheme during Sandholdt and Hames deposition.....	33
5. Possible load casts at the base of interbedded sandstones in the Sandholdt Member at measured section 8.....	38
6. Crossbedding in an interbedded sandstone in the Sandholdt Member at measured section 8....	38
7. Phosphoritic bed with light brown limestone concretions at measured section 191.....	55
8. Convolute bedding, load cast features, and pebbles of phosphate in a phosphoritic bed....	57
9. Load casts with pellets and pebbles of phosphate in a phosphoritic bed.....	57
10. Possible water escape structures in a thick phosphoritic bed.....	58
11. Resistant phosphoritic beds in the basal portion of the Hames Member.....	59
12. Oolite (T334-1) in white light showing at least five generations of growth indicated by light and dark brown rings.....	63
13. Oolite (T176) in polarized light showing concentrically oriented muscovite-illite laths.....	65

Figure	Page
14. Oolite (T176) in polarized light showing possible oriented quartz detrital grain.....	65
15. Pellet (T399-6) in white light showing grapestone or crude mosaic structure.....	69
16. Fuzzy pellet (T332-7) in white light with other pellets of various sizes.....	69
17. Pellets (T332-14) in white light showing included diatom debris.....	70
18. Pellet (T332-14) in white light showing a complete diatom included.....	70
19. Non-centered pellets (T96-5) in white light.....	74
20. Same as figure 19, but in polarized light to emphasize the similarity in size and shape of included grains and framework grains.....	74
21. Non-centered pellet (T96-5) in white light showing both protruding and intruding grains.....	75
22. Non-centered pellet (T332-7) in white light showing a protruding detrital grain.....	75
23. Plot of colophane determined petrographically with respect to P ₂ O ₅ content determined through geochemical analyses.....	79
24. X-ray diffraction patterns of oolite-dominated samples using nickel-filtered copper K α radiation at a scan rate of one degree 2 θ per minute.....	81
25. X-ray diffraction patterns of pellet-dominated samples using nickel-filtered copper K α radiation at a scan rate of one degree 2 θ per minute.....	82
26. Determination of CO ₂ content from $\Delta 2\theta_{(004)-(410)}$ of carbonate-fluorapatite.....	84

Figure	Page
27. Pellet (S108) with grain inclusion showing massive character of collophane.....	86
28. EDAX readout of pellet in figure 27 showing elemental composition of collophane.....	86
29. Pellet (S60-14) showing clustered material on probable diatom debris.....	87
30. EDAX readout of clustered material in figure 29 showing elemental composition.....	87
31. Model of phosphoritic rock genesis in the Robinson Canyon-Laureles Grade area.....	98
32. Model of transport and final deposition of the phosphoritic rocks in the Robinson Canyon-Laureles Grade area.....	99

Plate

1. Geologic Map of the Robinson Canyon-Laureles Grade Area.....	in pocket
2. Structure Sections.....	in pocket
3. Sample Locality Map.....	in pocket
4. Correlation of Measured Sections 467, 60, 8, 191, and 109.....	in pocket
5. Correlation of Measured Sections 259, 276, 399, and 332.....	in pocket

LIST OF TABLES

Table		Page
1.	Paleocurrent Indicators.....	16
2.	Checklist of Megafossils from the Robinson Canyon-Laureles Grade Area.....	23
3.	Checklist of Microfossils from the Robinson Canyon-Laureles Grade Area.....	40
4.	X-ray Diffraction Data of Siliceous Rocks.....	45
5.	Petrographic Data on Phosphoritic Rocks.....	61
6.	Semiquantitative Analyses of Phosphoritic Rocks.....	78

ABSTRACT

The stratigraphic sequence of the Robinson Canyon-Laureles Grade area in Monterey County represents at least two periods of deposition upon a pre-Cretaceous to Cretaceous crystalline basement. The oldest observable sedimentary unit is the middle Miocene or older Chamisal Formation which is composed of nonmarine and shallow marine sequences of rocks. Overlying the Chamisal Formation unconformably, is the middle Miocene to late Miocene Monterey Formation. The Monterey Formation represents a relatively deeper water marine sequence of rocks compared to the Chamisal Formation and is made up of rocks which were deposited in neritic, transitional outer neritic to middle bathyal, and lower middle bathyal depth environments. Interbedded with the transitional member of the Monterey Formation are pelletal phosphoritic rocks. Most of these phosphoritic rocks represent fecal pelletal material, formed in shallow-water environments, which was then transported by fluidized grain flows to much deeper water environments. The fecal material originally contained phosphorus and may have been enriched in phosphorus further by metasomatic processes. The paleogeography of the basin in which the Monterey sediments were deposited had characteristics of a continental borderland trough which was an ideal setting for the phosphatic enrichment of fecal material already rich in phosphorus.

INTRODUCTION

Purpose of Investigation

Several exposures of oolitic, pelletal, and pebbly phosphoritic rock have been reported previously in the Carmel Valley area of Monterey County (Galliher, 1931; Rogers, 1944; Brown, 1962; Gower and Madsen, 1964; and Dickert, 1970). Stratigraphically, these phosphoritic rocks are restricted to the lower portion of the Monterey Formation in beds ranging in age from middle to late Miocene. This study involves a detailed description of the stratigraphy and characteristics of different types of phosphoritic rock in the Carmel Valley area. It was felt that this study would add more knowledge on the phosphoritic rocks with respect to several features: stratigraphic restrictive nature of occurrence; difference in character of phosphorus constituents related to possible lateral or vertical occurrences in stratigraphy; final depositional environments; and possible mode(s) of formation.

Previous Studies

Previous general geological studies have been conducted in the Carmel Valley area by Trask (1926), Galliher (1930), Cassel (1949), Brown (1962), Bowen (1965), Clark, Dibblee, Greene, and Bowen (1974), and Graham (1976). Specific studies in the fields of geophysics (Sieck, 1964), groundwater

(Thorup, 1976), stratigraphy (Bramlette, 1946), and biostratigraphy (Kleinpell, 1938) also have been done in the study area.

Location and Accessibility

The Robinson Canyon-Laureles Grade area is situated in Carmel Valley. The area is located in the southeast sector of the 7 1/2' Seaside quadrangle and is framed by latitudes 36°32'30"N, 36°30'00"N, and longitude 121°49'00"W, which serve as the north, south, and western limits (fig. 1). The eastern limit of the study area is the Laureles Grade road (G20). The study area can be reached by driving east on Carmel Valley road (G16) off of Highway 1 near the city of Carmel. Access to different parts of the study area is provided by Robinson Canyon road, Tierra Grande drive, Laureles Grade road, and several unimproved, privately owned, dirt roads. The total area studied is approximately 25 km².

Geography

The study area is divided by the Carmel River into northern and southern areas. Each area has its own distinct geography which is a reflection of the underlying bedrock. The northern area is characterized by smoothly rounded, grass covered hills which range in elevation from 45m at the Carmel Valley floor to 400 m near the top of Laureles Grade road.

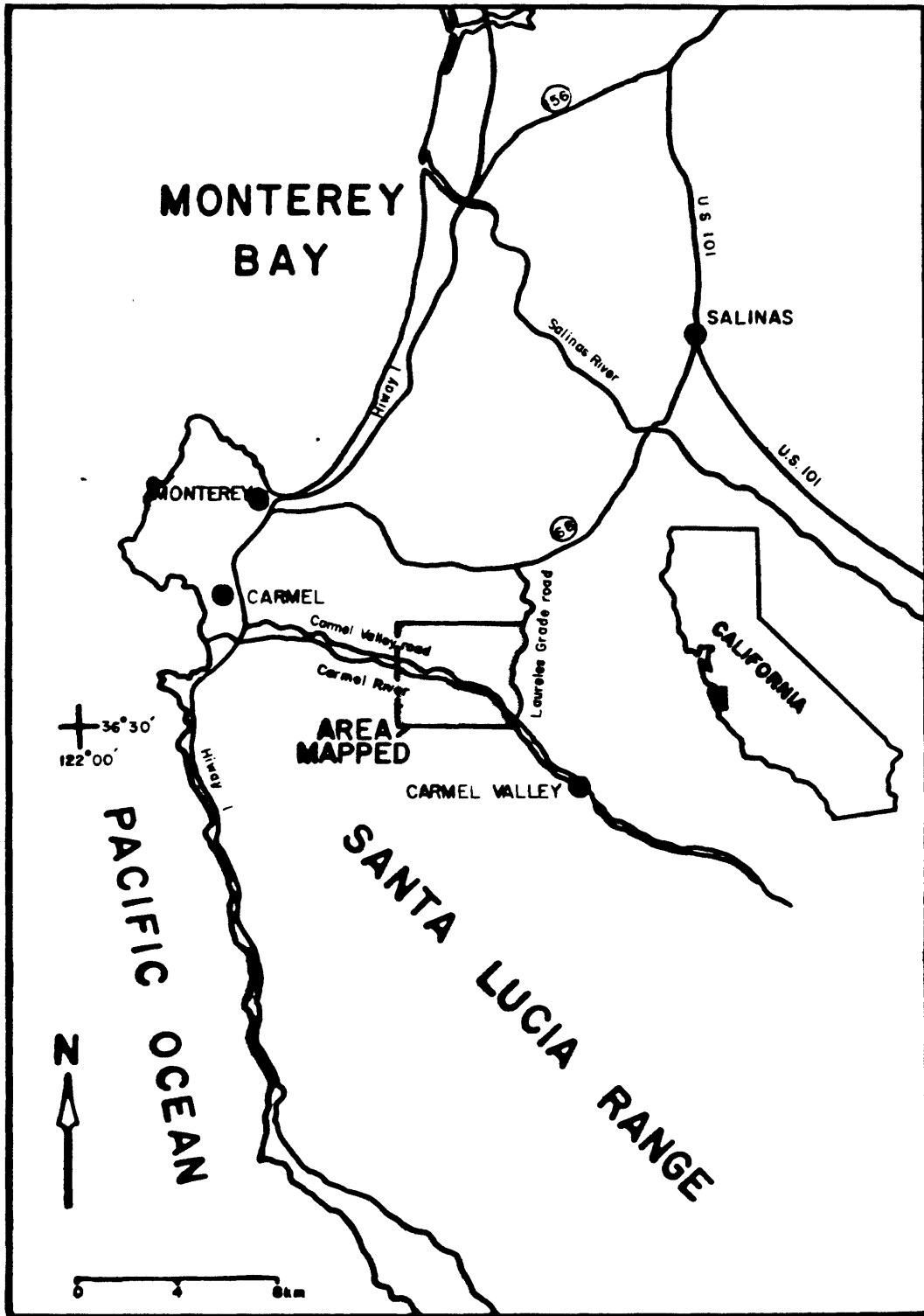


Figure 1. Location of the Robinson Canyon-Laureles Grade area.

Vegetation consists of tanoaks, chaparral, huckleberry and grassland. Hillsides and slopes are brushy, whereas hilltops and knolls are grassy and provide good range land for cattle. Wildlife consists of deer, rabbits, and snakes. The southern area differs from the northern area in being characterized by steep and rugged canyons which range in elevation from 45 m at the Carmel Valley floor to nearly 550 m on top of Snivley's Ridge. Vegetation ranges from very dense in the canyons to sparse on the hill tops and ridge lines. Redwoods, ferns, and a variety of vine plants grow in the canyons. Vegetation not restricted to the canyons includes oak trees, chaparral, and manzanita. Grasses predominate on the hill tops, and ridge lines. Wildlife consists of deer, rabbits and boar.

The north and south parts of the Carmel Valley have a moderate to mild climate. Rainfall is seasonal and is concentrated during the months of November through April; the annual average rainfall is 16-18 in.

Land use in descending order of area within the Carmel Valley is urban residential, pasture, and truck crops. The study area is predominantly used for pasture land, but housing developments have steadily increased on the Carmel Valley floor.

METHODS OF STUDY

Preliminary Investigation

A preliminary survey of all pertinent literature relating to the general geology of the study area was made before fieldwork was begun. A bibliography of regional geologic literature and specific literature on phosphate deposition was assembled, and then private-property ownership was surveyed and permits for trespassing were secured. Once permission had been obtained, a preliminary geologic investigation was made with the aid of aerial photographs.

Fieldwork

A total of 48 days was spent in the field, the majority of time being spent in the summer of 1977 and the spring of 1978. Fieldwork consisted of detailed geologic mapping of the study area plotted on a topographic map at a scale of 1:6,857. Older geologic maps were used for comparison, and in some cases added to or corrected. The final compiled map is shown on plate 1. An enlarged aerial photograph at a scale of 1:6,000 was utilized also as an aid for plotting and locating purposes. Detailed measured sections were made of rock exposures of reasonable accessibility showing the maximum measurable thickness with the least deformation, and the least weathering. Selective samples were taken from measured

sections for slabbing and thin section preparation, and for study of the megafossils and microfossils, phosphate content, and the total chemistry. Nomenclature used in describing measured sections is based on standard references (Wentworth grain size parameters; 1963 Geological Society of America rock color chart; Maurice Powers 1953 visual grain roundness determinations), and textural rock names used are those of C. M. Gilbert (in Williams, Turner, and Gilbert, 1954). Field presence of CaCO_3 was indicated by HCL; P_2O_5 presence was tested by a vanadomolybdate solution. Supplemental photographs were taken of selected measured sections. Laboratory work and procedures are described in Appendix 1.

STRATIGRAPHY

The Carmel Valley area is underlain by a crystalline basement that is overlain by sediment representing at least two major periods of deposition. Locally within the Robinson Canyon-Laureles Grade area, the first marine transgressive sequence started about middle, or possibly early Miocene time and is represented by the nonmarine-to shallow-marine-Chamisal Formation. A possible regressive phase, which may have occurred during late middle Miocene time, terminated deposition of the Chamisal Formation. The second marine transgressive sequence started during late middle Miocene time and is represented by the outer-littoral-to deep-water-marine Monterey Formation. Subsequently, the Monterey Formation was unconformably overlain on the Chamisal Formation and on granodiorite basement where the Chamisal Formation may have been stripped from or was never deposited on. Figure 2 is a generalized stratigraphic column of the study area.

Basement

The basement of the study area is made up of pre-Tertiary igneous and metamorphic rocks which constitute 15 percent of the total surface area. The first mention of igneous rocks in the Monterey-Carmel area was by Lawson (1893), who called the granitic rocks there the Santa Lucia Granite. The term Santa

		AGE	UNIT	THICKNESS	LITHOLOGY	COLUMN	
CENOZOIC	QUATERNARY	RECENT	Alluvium, Landslides	20	Sand, gravel, unconsolidated older material		
		PLEISTOCENE	Older Alluvium unconformity	10	Boulder, cobble conglomerate, coarse grained arkosic sandstone		
	TERTIARY	MIOCENE	MONTEREY FORMATION	Hames Mbr.	150	Siliceous claystone, porcelanite, less common shale interbeds, limestone concretions and beds, with thin phosphoritic beds at base of unit	
				Sandholdt Mbr.	80	Shale, siltstone, claystone, limestone, phosphoritic beds.	
		MIDDLE		Laureles Sandstone Mbr. unconformity	60	Medium to fine grained arkosic sandstone	
				LOWER?	Los Tularcitos Mbr.	100	Coarse to medium grained arkosic sandstone
		CHAMISAL FM.			Robinson Canyon Mbr. unconformity	115	Granule to very coarse, in part cobbly, pebbly, arkosic sandstone
	MESOZOIC	CRETACEOUS	Santa Lucia Granodiorite		Granodiorite		
	PALEOZOIC		Sur Series	10	Quartzofeldspathic schist		

Figure 2. Generalized stratigraphic column of the Robinson Canyon-Laureles Grade area (lithologic symbols explained on plate 4).

Lucia has since been applied by many workers to all types of granitic rocks included within the Santa Lucia Range. In response to this usage, Ross (1976a) proposed a more restrictive terminology, the prophyritic granodiorite of Monterey, to distinguish the Monterey-Carmel rocks from other granitic rocks within the Santa Lucia Range.

Granitic rocks noted by the author in the study area are granular, medium-grained, and biotite granodiorite to quartz diorite in composition. The average composition observed in stained samples is 5-10 percent K-spar, 15-20 percent quartz, 70-80 percent plagioclase, and 10-20 percent biotite. The predominant feldspars are plagioclase Ab⁷⁰ An³⁰ and microcline. Accessory minerals including magnetite and zircon also are present. Quartz shows consistent undulatory extinction. The granodiorite weathers moderate pink (5R7/4) to moderate reddish-orange (10R6/6) in color. Weathered products consist of rubble and very coarse sand.

Present within the study area, but not mapped because of insignificant size, are small outcrops of metamorphic rock belonging to an assemblage of rocks called the Sur Series Schists by Trask (1926). These outcrops occur only along the Laureles Grade road area. The predominant metamorphic rock is a quartzofeldspathic schist. This schist is similar to rocks called the Sierra de Salinas Schist by Ross (1976a) which occurs to the east of the study area. The schist weathers to a moderate reddish-brown (10R4/6) color.

If these metamorphic rocks in the study area are related to, or equivalent to, the Sierra de Salinas Schist, they may be Mesozoic in age (Ross, 1976a). The granodiorites which have intruded the metamorphic rocks are Cretaceous in age and range from 77 my to 106 my (Compton, 1966). A much more thorough discussion of the crystalline basement rocks of the Santa Lucia Range has been given by Compton (1966), Wiebe (1970), and Ross (1973, 1976a,b).

Chamisal Formation

The name Chamisal Formation was first proposed by Brown (1962) for exposures of arkosic sandstone of middle Miocene age overlying granodiorite basement and underlying the Monterey Formation in the Robinson Canyon vicinity. Trask (1926) originally assigned these sandstones to the Temblor Formation. Brown (1962) divided the Chamisal Formation into the nonmarine Robinson Canyon Member, the intermediate conglomeratic Chamisal Member, and the upper marine Chamisal Member. Identical rocks located southeast of the study area in the Jamesburg quadrangle were mapped as Vaqueros-Temblor sandstone by Fiedler (1944) and as the Cachagua Member of the Chamisal Formation by Neel (1963) and Wiedman (1964). Bowen (1965) proposed the name Los Tularcitos Member for Brown's intermediate and upper marine Chamisal members. Clark, Dibblee, Greene and Bowen (1974) lumped all marine sandstones

within the study area including the Laureles Sandstone into a "Middle Miocene Sandstone." Thorup (1976) considered all sandstone units in the area as the "Tularcitos", a name primarily intended to designate a single groundwater aquifer unit or zone.

The author has elected to use the name Chamisal Formation as originally proposed by Brown and the names Robinson Canyon Member to designate the lower nonmarine portion of the Chamisal Formation, and Los Tularcitos Member as proposed by Bowen (1965) to designate the intermediate and upper marine portions of the formation. The Laureles Sandstone is not included here in the Chamisal Formation and will be discussed under the Monterey Formation.

The type locality for the Chamisal Formation is located along Robinson Canyon, from the crest of Chamisal Ridge to the alluviated floor of Carmel Valley (Bowen, 1965). Brown (1962) reported a maximum exposed thickness of 290 m and showed a general thinning in a westerly direction. Within the study area the Carmel Valley test well (Appendix 2) indicated a possible thickness of at least 210 m for the Chamisal Formation.

Robinson Canyon Member

Distribution and Thickness. Outcrops of the Robinson Canyon Member constitute less than five percent of the total surface area mapped. Fair exposures occur on the flanks of an east-west-trending syncline in the southwest sector of the

study area (plates 1 and 2). The characteristic red colored portion crops out only at the mouth of Robinson Canyon within the study area. No exposures were found north of the Carmel River. The Robinson Canyon Member is easily erodible and forms an almost badland-type of topography in the south; exposures at the mouth of Robinson Canyon are the exceptions in that they are more indurated and fairly resistant.

A maximum exposed thickness of the member in the study area is approximately 30 m; the Carmel Valley test well, however, which reached granodiorite basement, shows a possible thickness of 115 m (Appendix 2). One mile south of Sniveleys Ridge, outside of the study area in the vicinity of Pinyon Peak, a maximum exposed thickness of 125 m with thinning in a westerly direction was reported for the member (Brown, 1962).

The basal contact of this member with granodiorite basement is exposed in only a few areas. One outcrop at the middle western edge of the study area shows a possible contact, but it is too poorly exposed for a definitive description of the type of contact.

Lithology. The Robinson Canyon Member is a granule to very coarse, in part cobbly, pebbly, arkosic sandstone. Rocks exposed in the southern part of Robinson Canyon are texturally identical to those in the north at the mouth of Robinson Canyon, but differ in lacking the red coloration and being less indurated. Fresh and weathered exposures in the south

exhibit a pale olive (10Y6/2) color, as contrasted with a fresh yellowish-gray (5Y7/2) to weathered moderate red (5Y4/6) coloration of northern exposures. All exposures are characterized by a somewhat salt and pepper color distribution and they weather to a coarse, sandy soil.

All rocks are composed of very coarse, poorly sorted, equant to tabular, angular, and subangular grains. Grain surfaces are dull and stained by iron oxides. Composition is predominantly quartz (50 percent), feldspars (40 percent), biotite (8 percent), and other ferromagnesium minerals. The Robinson Canyon Member is framework-supported and lacks clay- or silt-sized material. Ferruginous cement amounts to less than one percent of the total rock composition. Cobbles and pebbles dispersed within the member constitute less than one percent of the total rock. Included within this coarser fraction are grayish, mud-cemented, spherical concretions of coarse sand ranging from 2.5 cm to 5 cm in diameter; well rounded, 0.5 cm to 5 cm, biotite-schist clasts; abundant, rounded, 0.5 cm to 5 cm, quartz clasts; and a characteristic predominance of rounded to rectangular, 0.5 cm to 5 cm, pink feldspars. Where the member is fairly well indurated, cohesiveness appears to be the result of compaction.

Outcrops are generally massive, but where bedding does occur beds range in thickness from 1 m to 2 m. These beds are traceable for only 8 m to 10 m and consist of boulder to cobble conglomerates composed of well rounded to subangular

quartz diorite, gneiss, and schist clasts. Numerous, 7-cm-to 15-cm-thick by 3-m-to 5-m-long lenses of gravel to pebbly conglomerate made up of well rounded, 0.5 cm to 1 cm pebbles of granodiorite, schist, and quartzite, also are present.

Age and Correlation. No fossils were found in the Robinson Canyon Member; therefore, no precise age can be assigned. Judging by the gradational contact with the overlying Los Tularcitos Member, which contains Temblor stage (middle Miocene) invertebrate megafossils near the top, the upper part of the Robinson Canyon Member is considered to be at least early middle Miocene in age. The Robinson Canyon redbeds best correlate lithologically with the nonmarine, late Oligocene Berry Formation located farther to the south of the study area (Brown, 1962).

Depositional Environment. Because of the paucity of exposures of the Robinson Canyon Member within the study area, an interpretation of the depositional environment is greatly impeded. Despite this limitation, however, the author postulates that the Robinson Canyon Member is representative of an alluvial facies because of the following features. The source rock of the Robinson Canyon Member is considered to have been the granodiorite basement because of the predominance of quartz and feldspar in the sediment with the occurrence of granodiorite, gneiss and schist clasts. The basement is predominantly granodiorite, but does contain scattered

remnants of the Sur Series Schists. The poor sorting, angularity, and coarseness of the sediment with the occurrence of occasional conglomerates are indicative of the close proximity of source rock. Lenses of gravel and pebbles are suggestive of small channels; discontinuous boulder to cobble conglomerates possibly represent larger channels. The lack of clay matrix and abundance of feldspars may be indicative of either an arid or cold climate, but the red coloration of the member often is attributed to a warm, humid climate (Folk, 1974). Intrastratal oxidation (Walker, 1967), common in dry climates, however, could explain the development of these features. The red coloration strongly suggests a subaerial environment, as does the lack of marine fossils.

Sediment transport probably generally was southward. Paleocurrent indicators at localities 482 and 467 near the contact between the Robinson Canyon Member and the Los Tularcitos Member (table 1, plate 3) indicate transport southward. Paleocurrent data at locality 537 within the Los Tularcitos Member also indicate a southerly flow. A westerly component to the sediment transport is shown by paleocurrent indicators 453 and 509. The lack of Robinson Canyon Member to the north of the Carmel River, where perhaps it never was deposited, supports the idea of sediment transport to the south.

Los Tularcitos Member

Distribution and Thickness. The Los Tularcitos Member is exposed primarily on the south side of the Carmel River, predominantly in the southwestern sector of the study area, and along the northern edge of the Tularcitos Fault. A few scattered outcrops of the member occur north of the Carmel River, fairly close to the valley floor. The total exposed area of the member constitutes 20 percent of the study area. The topographic expression of the member varies due to differences in degrees of induration and coarseness. On the northward-facing flanks of Pinyon Peak, located directly south of Snivleys Ridge, just at and beyond the mid-southern edge of the study area, the Los Tularcitos Member exhibits a resistant, massive, cliff-forming, cavernous character. This same formidable character is exhibited in the southeastern extremity of the study area at the Garland Ranch Regional Park and along the northern side of the Tularcitos Fault. Along the fault are vertical cliffs with drops of 60 m which have been called the "Palisade Cliffs" (Thorup, 1976). Other less prominent outcrops occur in landslide areas flanking Robinson Canyon.

The thickness of the Los Tularcitos Member at the type locality of the Chamisal Formation is 120 m with a general thinning to the west (Brown, 1962; Bowen, 1965). The Carmel Valley test well (Appendix 2) shows a thickness of at least 100 m for the member. The Los Tularcitos Member is

considerably thinner north of the Carmel River where measured thicknesses range from 0 m to 30 m.

The character of the Los Tularcitos basal contact differs between north and south portions of the study area. To the south, the Los Tularcitos Member conformably overlies the Robinson Canyon Member and shows a gradual upward trend in decreasing grain size from very coarse to coarse to medium size, and a relative increase in calcium carbonate content. In some exposures a basal 1-m-to 2-m-thick zone is burrowed (fig. 3, plate 3). All these features are indicative of a change from nonmarine to marine conditions. To the north, the marine portion rests on a 3-m-thick, siliceous shale to claystone which in turn lies nonconformably on granodiorite basement.

Lithology. The Los Tularcitos Member is a coarse to medium grained, arkosic sandstone. Northern and southern exposures, excluding the Tularcitos Fault and Garland Ranch Regional Park areas, have identical characteristics. Fresh rock surfaces exhibit a very pale orange (10YR8/2) color and weathered surfaces show a dark yellowish-orange (10YR8/2) color. Grains are coarse to medium sized, equant shaped, and angular with somewhat rough surfaces. Sorting is fair to good. Feldspars (albite and microcline) and quartz occur in sub-equal amounts. Biotite grains, 0.7-mm-to 0.8-mm-long, occur in a few samples. The Los Tularcitos Member is predominantly framework-supported. Matrix material, when present, consists



Figure 3. Burrow structures in the basal portion of the Los Tularcitos Member at locality M-Y-471 (plate 3).

of micrite which normally amounts to less than two percent, but it increases toward the top of the member. Collophane cement is present in amounts less than two percent at the top of the member at localities T457 and T60-1. Pore space and degree of compaction are variable as reflected in geomorphic expression which ranges from friable, somewhat nonconsolidated material on hillsides to more highly indurated cliff exposures. Well rounded quartz, feldspar, and very friable, green clay pebbles 1 to 2 cm in diameter also are present in the sandstone. The member weathers into a coarse-medium grained, sandy soil.

The Los Tularcitos Member generally is massive in the vicinity of Robinson Canyon, and contains 0.5-m-thick, bioclastic, sandy, limestone beds at the top. In the bottom portion of the member, there are very large, calcareous, coarse-to medium-grained concretions up to 1 m by 1.5 m. These large concretions occur in a definite zone and are aligned parallel to bedding which is conformable with the underlying Robinson Canyon Member. They also show a definite decrease in size up section. At and within 2 m from the top of the member, there is a graded, boulder-cobble conglomerate. This conglomeratic zone consists of both well rounded and angular, 5-cm to 25-cm, granite, felsite, rhyolite, quartz, and quartzite clasts set in a very coarse, calcareous, sandy matrix. This composition is slightly different from that of conglomerates in the Robinson Canyon Member. The capping

conglomerate zone ranges from 3 m to 5 m in thickness. A similar conglomerate on Pinyon Peak due south and outside of the study area was reported by Brown (1962), who also noted the difference in composition between this conglomerate and others in the underlying Robinson Canyon Member. He postulated that these conglomerates are related to the Paleocene Carmelo Formation, but this has been shown by stratigraphic studies to be impossible. Graham (1976) suggested the possibility that this material may have come from the late Oligocene to early Miocene (Zemorrian) Pinnacles Formation.

Outcrops along the Tularcitos Fault and in the Garland Ranch Regional Park are much coarser than those in the Robinson Canyon vicinity. Because marine fossils similar to those in the Los Tularcitos Member have been recovered from these coarser rocks at the northwestern extremity of the Tularcitos Fault, the name Los Tularcitos Member was applied to these outcrops despite the differences in lithology compared to outcrops along Robinson Canyon. These coarse exposures are predominantly conglomerates with sandy interbeds. The conglomerates consist of poorly sorted, angular, 0.5 cm to 20 cm, rhyolite, granite, and schist clasts set in a matrix of coarse to very coarse, angular, feldspar and quartz grains.

Age and Correlation. All fossil localities in the Los Tularcitos Member are near or at the top of the marine member. Brown (1962) reported fossils within 45 m of the base, but

also noted the greater abundance of fossils near the top of the member. Locations of megafossils shown on table 2 are plotted on plate 3. The most common guide fossil in the Los Tularcitos Member is the Pecten andersoni Arnold. Most pecten localities are in Robinson Canyon and to the north at locality M-Y-60-1. Northern sandstone outcrops at localities M-Y-216 and M-Y-228 were assigned to the Los Tularcitos Member rather than the Laureles Sandstone because they are more indurated compared to the later sandstone unit. These northern sandstone outcrops have a feldspar/quartz ratio of 1:1, a burrowed zone comparable to those overlying the Robinson Canyon Member, and the pelecypod Arca montereyana Osmont, one of the more typical guide fossils of the Los Tularcitos Member (Bowen, 1965). Fossils occur in bioclastic, sandy, limestone beds near the top of the member. All fossils indicate a middle Miocene age for the Los Tularcitos Member.

The Los Tularcitos Member best correlates lithologically with the lower Miocene Vaqueros Formation located to the south of the study area. This suggests the possibility that the Los Tularcitos Member is a time-transgressive equivalent of the Vaqueros Formation (Brown, 1962).

Depositional Environment. The similarity in composition and the conformable gradational basal contact with the Robinson Canyon Member indicate that the underlying nonmarine member was the source rock or that both that unit and the marine

Los Tularcitos Member were derived from the same source. Based on megafossil content, however, the Los Tularcitos Member is believed to have been deposited in a shallow-marine environment. The more conglomeratic beds along the Tularcitos Fault and in the Garland Ranch Regional Park probably were deposited in transitional nonmarine to marine environments.

Paleocurrent data observed at localities 482, 467, and 537 (table 1, plate 3) indicate sediment dispersal from north to south. A possible westerly component is shown by paleocurrent indicators at 453 and 509.

Monterey Formation

Blake (1855) proposed the name Monterey Formation for rocks of Tertiary age on a hill two miles southeast of the town of Monterey. Lawson (1893) used the name Monterey series as a group name for rocks of Miocene age near Carmel. Galliher (1932) formally established the name Monterey Formation and designated the type locality which is a composite section made up of several outcrops near the town of Monterey. He further divided the formation into 5 members exclusive of a basal sandstone, based upon lithology and microfaunal zones. In 1938, Kleinpell studied the Monterey Formation at Reliz Canyon on the west side of the Salinas Valley, subdividing it into stages based on benthonic Foraminifera. Bramlette (1946) studied the Monterey Formation and restricted the

name to strata of Miocene age characterized by an unusually high proportion of silica covering a wide regional area extending from just north of San Francisco to slightly south of Los Angeles. Cassel (1949) studied the Monterey Formation adjacent to and east of Galliher's area. He separated the siliceous portion of the formation into four units and introduced the name Laureles Sandstone Member for a basal sandstone unit. Bowen's (1965) study of the Monterey and Salinas quadrangles resulted in a three-member division of the formation consisting of a basal member called the Laureles Sandstone after Cassell (1949), a middle siliceous-shale porcelanite called the Aguajito Shale Member, and a locally capping unit called the Canyon Del Rey Diatomite Member. Graham (1976) subdivided the Monterey Formation into two parts based on Durham's (1974) lithological division of the Monterey Formation in the Salinas Valley. These divisions are a lower calcareous mudstone called the Sandholdt Member and an upper siliceous shale to porcelanite sequence called the Hames Member. Graham considered the Laureles Sandstone a sub-Monterey sandstone, and included it within a Middle Miocene Sandstone category.

The Monterey Formation in the study area consists of a basal sandstone, a transitional sandy shale and claystone unit which is in part calcareous, and a siliceous shale and porcelanite unit. The basal sandstone unit is much finer

grained and more friable than the Los Tularcitos Member of the Chamisal Formation and is here assigned the name Laureles Sandstone as proposed by Cassell (1949). The transitional calcareous unit and overlying siliceous unit are assigned the names Sandholdt Member and Hames Member respectively based on the lithologic similarity to Durham's (1974) members of the Monterey Formation.

The Monterey Formation is exposed over 50 percent of the surface area studied. It is at least 300 m thick on the northern edge of the area (Sieck, 1964; Ross and Brabb, 1973). Within the general Monterey-Carmel area, however, the Monterey Formation may be as thick as 900 m (Bowen, 1965; Cassell, 1949), 1000 m (Galliher, 1930), 1050 m (Kleinpell, 1938) or 1100 m (Bramlette, 1946). The differences in thickness reported are due primarily to post-depositional erosion of the uppermost portion of the unit.

Laureles Sandstone Member

Distribution and Thickness. The Laureles Sandstone is exposed primarily in the eastern portion of the study area, but it also occurs as a thin veneer overlying the Chamisal Formation in the southwest. The total outcrops of the Laureles Sandstone, however, account for less than two percent of the surface area studied. This basal Monterey sandstone is a very friable, non-resistant slope-former having a maximum exposed thickness of 40m in Juan de Matte Canyon to a minimal

3-m-thick blanket to the southwest. Bowen (1965) reported a thickness of 60 m at the type locality at the northeastern edge of the study area. Neel (1963) and Wiedman (1964) have mapped this sandstone unit to the southeast of the study area and noted a maximum thickness of 200 m.

The Laureles Sandstone overlies granodiorite basement north of the Carmel River and overlies the Chamisal Formation to the southwest. In some exposures, a friable, pebbly, very coarse grained basal Laureles Sandstone with well-rounded pebbles occurs in sharp nonconformable contact with granodiorite. The contact between the Laureles Sandstone and the Chamisal Formation to the southwest probably is unconformable. The Los Tularcitos Member is capped by a 3-m-to 5-m-thick conglomeratic zone which overlies a predominantly calcareous, coarse-to medium-grained sandstone. This conglomerate separates the Los Tularcitos Member of the Chamisal Formation from the overlying Laureles Sandstone. Bowen (1965) noted the abruptness in graduation from the Los Tularcitos Member to the Laureles Sandstone and used this as one of his criteria to differentiate between the two sandstones. Bone beds, which have been closely related to major and minor unconformities and submarine diastemic surfaces (Carozzi, 1960), occur at or near the contact between the two sandstones. These features all suggest that the Laureles Sandstone rests unconformably on the Chamisal Formation.

Lithology. The Laureles Sandstone Member is a friable, medium-to fine-grained, arkosic sandstone. This basal Monterey sandstone changes little in character between north and south exposures within the study area. Outside the study area, lithological differences also evidently are minimal (Neel, 1963; Wiedman, 1964). Fresh and weathered exposures differ in color from the base to the top of the member. Fresh basal sandstones have a yellowish-gray (5Y7/2) color and weather to a grayish-yellow (5Y8/4) color; both fresh and weathered color distributions are homogeneous. The top portion of the member has a fresh yellowish-gray (5Y8/1) color and weathers to a very light gray (N8) color; both of these fresh and weathered color distributions are homogeneous also. Sandstone grain sizes change from medium to fine upward, whereas laterally there is a fining northward along Juan de Matte Canyon. Sandstone in the southwest part of the study area, which overlies the Chamisal Formation, is fine grained. Grains are well sorted, equant, and subangular to subrounded with mostly smooth surfaces. This sandstone is composed of about 50 percent quartz and 50 percent feldspar; the latter shows considerable sericitization. Biotite is fairly common and accounts for one to three percent of the rock. Brown (1962) noted subangular phosphatic clasts and phosphatic matrix in the Laureles Sandstone in the San Jose Creek area just southwest of the study area. At measured

section 259 (plate 5) the upper part of the sandstone contains a little phosphate. Two meters above this member, within the Sandholdt Member, a high concentration of phosphoric pellets is present in boulders of coquina at section 259. The small amount of matrix, which increases up section, consists mostly of clay material. Calcium carbonate cement ranges from minimal at the base to abundant at the top of the sandstone near fossil beds. The sandstone is framework-supported, very friable, loosely compacted, and porous. At one outcrop, where this sandstone overlies granodiorite basement, the sandstone is coarse grained, very friable, and contains abundant, well-rounded pebbles of granitic and felsitic material up to 1 cm in diameter.

The Laureles Sandstone generally is massive in appearance. Bedding rarely occurs and is indicated by poorly-to well-cemented fossil zones made up of discontinuous, 0.5-m-thick lenses of bone debris and pelecypod coquinas. The coquinas are characterized by whole articulated specimens lining the bottom of beds overlain by smaller, less densely packed, disarticulated specimens. Encompassing the bone and shelly debris is fine-grained sandstone cemented by calcite. The sandstone member weathers into a fine, sandy soil.

Age and Correlation. No microfossils were recovered from the Laureles Sandstone within the study area. In measured section 467 (plate 4), microfossils within the

Sandholdt Member directly overlying the Laureles Sandstone indicate a Luisian age; therefore, the Laureles Sandstone is Luisian or older in the study area.

Megafossils restricted to the upper portion of the Laureles Sandstone are shown on table 2. Of particular interest are concentrations of whale bones in zones at the top of the member. These zones show a decrease in size of individual bones in a southerly direction. Also present are invertebrate megafossils which form coquinas. Chione sp? makes up nearly 90 percent of the fauna, and in many beds, the two valves are articulated. Identical coquina zones were reported by Neel (1963) who also noted that Chione sp? often was articulated. He called these fossil-rich zones reefs.

The Laureles Sandstone Member cannot be correlated with any other formation exposed nearby other than those mentioned by Neel (1963) and Wiedman (1964). It appears to be a localized depositional unit rather than a unit of regional extent.

Depositional Environment. At the Tularcitos Guard Station just southeast of the study area, Graham noted that the massive, fine-grained Laureles Sandstone grades upward into the calcareous Sandholdt mudstone which contains an upper-middle bathyal foraminiferal fauna. This sequence in turn overlies the much shallower marine Chamisal Formation. The same situation occurs in measured section 467 (plate 4). At this section, microfossils in the Sandholdt Member

immediately overlying the Laureles Sandstone and within 2 m of the contact between the two, compose a Luisian fauna characteristic of upper bathyal depths. Directly below the thin Laureles Sandstone and within 9 m of the aforementioned microfossil locality is a much shallower water sequence represented by the Los Tularcitos Member. Phosphatic debris and matrix also occur in the Laureles Sandstone.

The author postulates that the Laureles Sandstone represents a condensed sequence which was deposited in shallow water as shown by the invertebrate megafossils. This interpretation is supported by the previously mentioned bone beds, foraminifera data reported by Graham (1976), forams found in measured section 467, presence of collophane matrix, and the type of contact with the underlying Tularcitos Member.

Sandholdt Member

Distribution and Thickness. The Sandholdt Member of the Monterey Formation is exposed in the northern portion of the study area and also as a thin veneer covering the Chamisal Formation to the southwest. The member is exposed over less than five percent of the area studied, but is of great importance with respect to phosphate deposition. The Sandholdt Member consists of sandy shale and massive claystone, and is transitional between the underlying Laureles Sandstone and the overlying more siliceous porcelanite portion of the Monterey Formation. This non-resistant to semi-resistant, gentle

slope-forming unit ranges in exposed thickness from 80 m in the central and western portions of the study area to 9 m in the southwest; along Laureles Grade road there is none. The unit thins both eastward and southwestward as does the Laureles Sandstone.

The basal contact of this member differs at different localities. In the central portion of the study area the member overlies a 3-m-thick, siliceous shale and claystone zone which in turn, overlies a granodiorite basement with an irregular, nonconformable contact. The Sandholdt Member is in fault contact with granodiorite farther to the southeast at BM 236. The exposed basal contact with the underlying Laureles Sandstone to the east and southwest is conformable and gradational, and is accompanied by 30-cm-to 50-cm-thick, bioclastic to massive limestone beds and concretions in both members near the contact. In the north-central portion of the study area, the Sandholdt Member conformably overlies and also underlies the Hames Member. At this locality, the basal contact is characterized by limestone beds and concretions as is the upper contact with the Hames Member. This shows that both the Sandholdt and Hames members interfinger (fig. 4). The basal contact with the underlying Chamisal Formation at measured section 60 (plate 4) indicates a very abrupt change from fossiliferous, resistant, medium-grained Chamisal sandstone to Sandholdt claystone which suggests that it is unconformable.

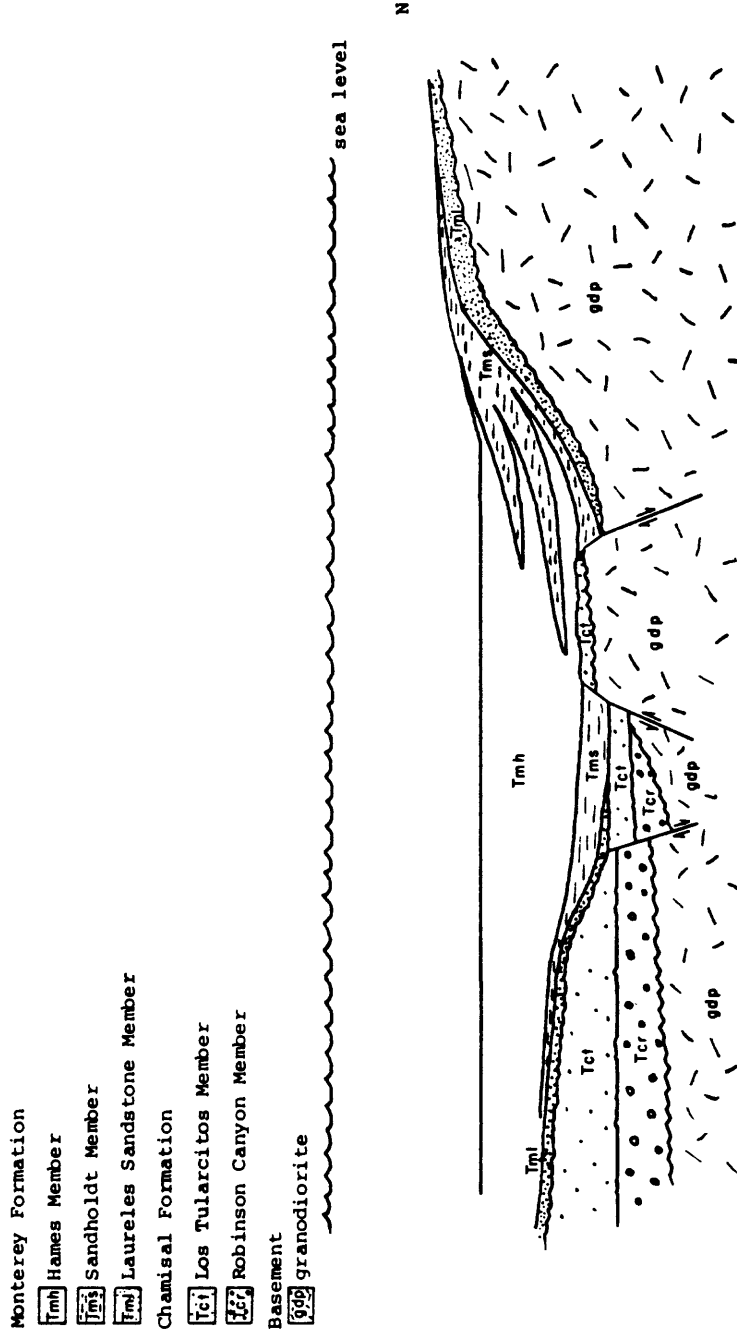


Figure 4. Sedimentation scheme during Sandholdt and Hames deposition.

Lithology. The Sandholdt Member consists of several rock types, which may represent local depositional environments. Types represented include massive claystone, shale, interbedded sandstone and limestone, and phosphoritic beds.

Massive claystones occur in the northern, eastern, and southern exposures of the Sandholdt Member and are present wherever the Sandholdt Member overlies the Laureles Sandstone. The claystone, however, is not restricted to the base of the Sandholdt, but occurs in zones throughout the member and in some outcrops, is the predominant lithology.

Fresh claystone exposures differ in color with respect to locality, but generally they are mottled, very light gray (N8) weathering to grayish-orange (10YR7/4). Petrographically the claystone is predominantly composed of clay sized, siliceous material with less frequent, angular to subangular quartz, feldspar, and chert grains 0.1 mm in diameter. Large planktonic foraminifers are common. Claystones are bioturbated; whole crabs, crab appendages, and undestroyed burrows occur in these bioturbated claystones. Some outcrops contain minor amounts of phosphate which probably is in the form of scattered phosphatic, organic, debris-like fish remains and phosphate pellets in the claystones. Claystones weather into a powdery, clayey soil. Claystone generally is massive, but also occurs in 5-cm-to 7-cm-thick beds separated by 1-cm-thick shale, bentonite-volcanic ash, and/or gypsum beds. The

gypsum is probably secondary in origin as indicated by its discontinuous bedding and veinlets which cut across claystone and shale bedding and the presence of deep-water foraminifers which indicate an environment unlikely for the formation of gypsum. The claystone generally grades into shale.

The shale is very friable and sporadically dispersed within the Sandholdt Member. The thickness of individual shale zones ranges from 5-cm-thick interbeds within claystone lithology to 5-m-thick beds higher in the section. The thickest zones of shale are in the central portion of the study area. Toward the northeastern edge of the study area, shale is minimal or absent, and in some of the eastern localities the Sandholdt Member is missing. Shale also increases upward through the Sandholdt Member. The color of the shale varies considerably depending on the amount of organic debris, silt, and fine sand present. Fresh shale color ranges from grayish-orange-pink (5YR7/2) to very pale orange (10YR8/2) and weathers to very pale orange (10YR8/2). Light brown (5YR5/6) banding or staining is fairly common.

Shales also are characterized by 1-to 2-mm-thick, alternating layers of clay and silt to very fine sand, and by distinct layers of foraminifers. Silt to fine sand layers are framework-supported and composed of well sorted, angular to subangular, grains of quartz and feldspar about 0.05 mm in

diameter which are cemented by calcite and some collophane. Foraminifers are calcite-filled and they lie flat within laminations. Flat lying biotite flakes are fairly common in clayey laminations. Glauconite is present in scarce amounts. A possible paleocurrent indication from a ripple-like structure at locality 191 within shale indicates flow from SW to NE. The shale weathers into a fine sandy, clayey soil. Where the shale is sandwiched between claystones its top and bottom contacts are gradational.

Interbedded sandstones within the Sandholdt Member are less common, but very distinct in outcrops. Exposures of interbedded sandstone occur only in the central portion of the study area. The most notable exposures are in measured section 8 (plate 4). The thickness of individual sandstone beds ranges from 5 cm to 1 m. Sandstone beds at section 8 show a definite thinning up section. Fresh sandstones are pale yellowish-orange (10YR8/6) and weather to grayish-orange (10YR7/4). Their color is fairly homogeneous, but streaking and staining are common.

The sandstone beds are massive, graded, and composed of grains which are fairly to poorly sorted, equant shaped, angular to subangular, and 0.1 mm to 0.2 mm in size. Sandstones range from matrix-to framework-supported. Framework constituents are composed of feldspar, quartz, fairly large amounts of biotite, muscovite, scarce phosphate pellets, and glauconite. Cements are calcite, iron oxides, and some

collophane. Matrix is predominantly siliceous, clay-sized material; the amount of matrix is quite variable. The sandstone weathers into a fine sandy soil. Basal contacts of individual sandstone beds are sharp and undulatory, possibly due to the development of load casts (fig. 5). Cross bedding is present in some sandstones (fig. 6) and indicates southward flowing paleocurrents. Where sandstone beds are not truncated, individual beds grade upward into shale. The sequential characteristics of these sandstone beds are very much like turbidites and conform to Bouma's (1962) A and B divisions.

Discontinuous limestone beds and concretions in the Sandholdt Member are not laterally or vertically restricted. Discontinuous limestone beds range in thickness from 8 cm to 50 cm. Flat, elliptical concretions range from 8-cm-to 30-cm-thick by 40-cm-to 2-m-wide, and are elongated along bedding. These very resistant beds and concretions have a dark yellowish-orange (10YR6/6) color when fresh and weather to a light brown (5YR5/6) color. Beds and concretions generally are structureless, aphanitic, and composed of calcite, quartz, and some dolomite. In contrast to the aphanitic variety of limestone, are limestones at measured section 259 (plate 5). These rocks are composed of recrystallized and well-cemented shelly coquinas with abundant pelletal phosphate. Limestones near the middle of measured section 191



Figure 5. Possible load casts at the base of interbedded sandstones in the Sandholdt Member at measured section 8.



Figure 6. Crossbedding in an interbedded sandstone in the Sandholdt Member at measured section 8.

(plate 4) are composed of concentrated, cemented, and recrystallized Foraminifera tests. Bones occur embedded in limestone concretions at measured section 399 (plate 6). The degree of silicification and dolomitization in limestone samples is quite variable. Contacts between limestone and other lithologies within the Sandholdt Member are very sharp.

Age and Correlation. Megafossils in the Sandholdt are uncommon and predominantly occur in the claystone beds. Fish remains and complete crabs, however, were found in a good state of preservation, and one gastropod encrusted by a barnacle was found at locality M-Y-256. Possible Scolicia and Parahantzchelinia trace fossils belonging to the Chondrites-Nereites assemblage were found within a phosphoritic bed at locality M-Y-332-6. The complete megafauna is listed on table 2. Microfossils from the Sandholdt Member listed on table 3 primarily occur in shale, but also in claystone and mudstone. The age of rocks ranges from Luisian in the southwest and north exposures, to late Luisian to Mohnian in central exposures, to late Mohnian in the southeast exposures.

The Sandholdt Member in the study area is readily correlated with Durham's (1975) Sandholdt Member of the Monterey Formation in the Salinas Valley area. Lithologies are very similar. Both are calcareous mudstones which contain siltstone and shale, abundant Foraminifera, thin sandstone interbeds, pelletal phosphoritic rocks, minor bentonite/volcanic

Table 3. Checklist of microfossils from the Robinson Canyon-Laureles Grade area (all microfossils collected by the author were identified by Kristin A. McDougall).

SPECIES	AGE AND LOCALITY												
	Luisian						Mohrian						
	Middle			Upper			Lower			Upper			
<i>Bolivina advena</i> Cushman													
<i>Bolivina advena</i> var. <i>striatella</i> Cushman	F	C											
<i>Bolivina brevior</i> Cushman													R
<i>Bolivina californica</i> Cushman	F												
<i>Bolivina floridana</i> Cushman			C										
<i>Bolivina mediceensis</i> Cushman						P							
<i>Bolivina parva</i> Cushman and Galliher							MR	MR					
<i>Bolivina rankini</i> Kleinpell												C	R
<i>Bolivina salinasensis</i> Kleinpell				A									
<i>Bolivina</i> cf. <i>B. seminuda</i> Cushman	F	A											
<i>Bolivina seminuda</i> var. <i>foraminata</i> Stewart and Stewart								R					
<i>BOLIVINA</i> <i>ticca</i> Kleinpell												A	R
<i>Bolivina tumida</i> Cushman						P							
<i>Bolivina</i> sp.		C	R			C	F						
<i>Bulinina galliheri</i> Kleinpell							F	F				F	F
<i>Bulinina montereyana</i> Kleinpell	F	R	R							A		A	F
<i>Bulinina montereyana</i> var. <i>delmonteensis</i> Kleinpell						C	F					C	R
<i>Bulinina ovata</i> d'Orbigny					P								
<i>Bulinina pseudotorta</i> Cushman							P						
<i>Bulininella curta</i> Cushman	C	F	C			C	F	P	C	R	A	A	C
<i>Bulininella dubia</i> Barbat and Johnson		R	C	R				R	F	R			R
<i>Bulininella elegantissima</i> (d'Orbigny)	F	F	F	A	A	P					C	A	
<i>Bulininella subfusiformis</i> Cushman								P	R	VR			
<i>Bulininella</i> sp.							F						
<i>Concavella gyroldinaformis</i> (Cushman and Goukoff)				R		C						F	F
<i>Epistominella gyroldinaformis</i> (Cushman)								P					
<i>Epistominella pontoni</i> (Cushman)	C	C	F	F	F						F		
<i>Epistominella reliziana</i> (Kleinpell)							R						
<i>Epistominella subperuviana</i> (Cushman)					P								
<i>Eponides exigua</i> (brady)										F	F	R	
<i>Eponides multicameratus</i> Kleinpell	F						F	F					
<i>Flofilus boueanus costiferus</i> (Cushman)								P	P				
<i>Fursenkoina californiensis</i> (Cushman)			F	A	C	C				C	F	F	
<i>Fursenkoina delmonteensis</i> (Cushman and Galliher)													C
<i>Fursenkoina</i> cf. <i>F. chreibersana</i> (Czjzek)							F	F					F
<i>Globigerina bulloides</i> d'Orbigny									F	V	R		
<i>Hemicristellaria beali</i> (Cushman)					P								
<i>Lenticulina</i> sp.	F												
<i>Marginulina beali</i> (Cushman)	F												
<i>Nonion costiferum</i> (Cushman)					P					A	A		C
<i>Nonion incisum</i> (Cushman)										R			
<i>Nonion</i> aff. <i>N. medio-costatum</i> (Cushman)													R
<i>Nonion montereyanum</i> var. <i>carmeloensis</i> (Cushman and Galliher)													R
<i>Nonion pizarrensis</i> Berry										R			C
<i>Nonion pizarrensis</i> var. <i>multicameratum</i> Cushman and Kleinpell													F
<i>Nonionella costiferum</i> (Cushman)	F	R	F			F	A	A			A	F	
<i>Nonionella miocenica</i> Cushman	F			A	F	A	F	P	C	R	R	A	A
<i>Pseudononion</i> n. sp. (Casaell)										R	F		
<i>Pulvinulinella gyroldinaformis</i> (Cushman and Goukoff)													C
<i>Pulvinulinella pacifica</i> Cushman													
<i>Robulus</i> aff. <i>R. monnensis</i> Kleinpell										R			
<i>Sugardina</i> n. sp. (Casaell)										R			
<i>Uvigerina carmelensis</i> Cushman and Kleinpell												F	
<i>Uvigerina</i> aff. <i>U. hanna</i> Kleinpell													VR
<i>Uvigerina</i> cf. <i>U. joaquinensis</i> Cushman									P				
<i>Uvigerina joaquinensis</i> Cushman					F	R							
<i>Uvigerina modeloensis</i> Cushman												R	
<i>Uvigerina</i> sp.													VR
<i>Uvigerinella californica</i>									P				
<i>Uvigerinella californica parva</i> (?) Kleinpell						P							
<i>Valvulinera californica</i> Cushman	C	A											
<i>Valvulinera californica</i> var. cf. <i>V. miocenica</i>									P				
<i>Valvulinera californica</i> var. <i>obesa</i> Cushman									P				
<i>Valvulinera miocenica</i> Cushman					A	P							R
<i>Valvulinera</i> sp.											F		R
<i>Virgulina californiensis</i> Cushman										C	F		
<i>Virgulina californiensis</i> var. <i>grandis</i> Cushman and Kleinpell										A	F		F
<i>Virgulina californiensis</i> var. <i>ticensis</i> Cushman and Kleinpell											F		A
<i>Virgulina delmonteensis</i> Cushman and Galliher									P	R	F	R	R
<i>Virgulina</i> aff. <i>V. delmonteensis</i> Cushman and Galliher													R
Diatoms contained in phosphatic pellets found by Rogers (1944) at localities MF-R-1 and MF-R-2 and identified by G. D. Hanna													
<i>Chaetoceros</i> sp.													
<i>Coccolodiscus</i> sp.													
<i>Podocira</i> sp.													
<i>Rhizosolenia</i> sp.													
<i>Stephanopyxis turris</i> sp.													

ash beds, dolomitic carbonate beds and ellipsoidal concretions, and fish and crab remains. Durham's Sandholdt Member, however, is Relizian to Luisian in age, whereas the member in Carmel Valley is Luisian to Mohnian in age. Durham's Sandholdt Member also is considerably thicker, but despite these differences, the author feels the correlation is valid and supported by a strong similarity in lithology. The Sandholdt Member in Carmel Valley, although a little younger, probably was deposited under similar environmental conditions as that in the Salinas Valley.

Depositional Environment. A consistent deepening trend with decreasing age is seen in the Sandholdt Member. Luisian mudstones contain Foraminifera indicative of upper bathyal, 200-600 m (based on Arnal, 1976), depths (Appendix 3). Late Luisian to early Mohnian outcrops contain Foraminifera indicative of 100-200 m depths, but they occur in turbidite beds along with some outer neritic species showing signs of transport (McDougall, 1978), so these fossils probably do not indicate true paleodepths. Some early Mohnian rocks contain Foraminifera indicative of upper middle bathyal, 500-1500 m, depths, and late Mohnian samples have Foraminifera indicative of lower middle bathyal, 1500-2000 m, depths. Turbidite beds at measured section 8 decrease in thickness up section and thus suggest deepening water conditions due to either subsidence or transgressive conditions. The megafossils indicate much shallower conditions than the Foraminifera, but

these fossils may have been transported. The presence of possible Chondrites-Nereites assemblages in phosphoritic beds are indicative of pelagic muds in deep bathyal environments (Seilacher, 1967). The good preservation of fish is indicative of low-oxygen environments typical of middle bathyal depths in slope environments which may correspond to the oxygen minimum zone. The presence of glauconite also is indicative of low-oxygen environments and slope environments.

The thinning of the Sandholdt Member to the southwest and east may be a function of either more distal sedimentation or possibly the result of onlapping onto relatively higher areas compared to centrally located deeper areas which contain thicker deposits. The latter case seems stronger. Brown (1962) noted Mohnian microfossils at the base of the Monterey Formation on Pinyon Peak just to the south of the study area. This finding indicates that the Monterey Formation becomes younger further south. The thinness of the Sandholdt Member south of the study area could have resulted from onlapping onto a relatively higher area compared to thicker sections which resulted from deposition in a deeper northern area located in the central portion of the study area. The decrease in age of the Monterey Formation to the east would likewise indicate that the thinning of the Sandholdt Member in that direction probably resulted from onlapping onto a paleohigh area. The author feels that the Sandholdt Member was deposited in upper bathyal or greater depths characteristic of upper or middle slope environments. Deposition may

have been partly in oxygen-poor waters and somewhat confined by possible barriers which existed to the south and east in the form of paleohigh areas which may or may not have been subaerially exposed during middle Miocene time.

Hames Member

Distribution and Thickness. The Hames Member constitutes over 50 percent of the surface area studied; the majority of exposures are on the north side of the Carmel River. The maximum exposed thickness is approximately 150 m.

The Hames Member generally overlies the Sandholdt Member conformably. The two units are gradational, the basal contact of the Hames not always being distinct. Where the Hames Member overlies the Laureles Sandstone, the contact is fairly abrupt between the sandstone and the overlying siliceous claystone and porcelanite.

Lithology. The Hames Member is composed of thin bedded, siliceous claystone, porcelanite, and rare chert with localized thin interbeds of shale, limestone blebs, and very thin interbeds of leached and non-leached pelletal, phosphoritic material. The terms porcelanite and chert as used here are defined by Murata and Larson (1975); namely, chert is a relatively pure silica rock which is dense and vitreous and consists mainly of chalcedony; porcelanite is softer, less dense, and less vitreous than chert and is characterized by

minute pore spaces which result in a dull matte luster resembling that of unglazed porcelain. Both chert and porcelanite can be either cristobalite (opal-ct) or quartz in composition. A third rock type, siliceous claystone, is included by the author. This rock type may have considerable impurities which give it the dullest luster and least density of the three rock types.

The porcelanite has a fresh very light gray (N8) to grayish-orange pink (5YR7/2) color and weathers to a light brown (5YR5/6) color. The siliceous claystone has a fresh very pale orange (10YR7/4) color and weathers to grayish orange (10YR7/4). Both types of rocks are somewhat banded. Chert, which is rare, consists of only very thin, discontinuous interbeds within porcelanite. These interbeds occur only south of the Carmel River. The chert has a fresh and weathered translucent pale brown (5YR5/2) color which is homogeneous in color distribution.

The porcelanite and claystone are cryptocrystalline except for occasional scattered Foraminifera casts and rare detrital quartz and feldspar grains. X-ray examination of claystone, porcelanite, and chert samples show a range in composition from cristobalite to predominantly poorly crystallized quartz (table 4). Porcelanite samples overlying turbidite sequences within the Sandholdt Member have X-ray diffraction patterns of quartz with fairly low crystallinity

Table 4. X-ray diffraction data showing composition and crystallinity of siliceous mudstone, porcelanite, and chert from the Hames Member in the Robinson Canyon-Laureles Grade area.

Sample	Type of rock	Cristobalite D(101)A	Quartz Crystallinity Index
96-2	porcelanite		3.24
466	chert		1.0
466	porcelanite	4.0767	1.0
60-16	mudstone		3.91
335	porcelanite	4.0860	1.0
389	porcelanite	4.0804	
458	porcelanite	4.0767	
253	porcelanite	4.0767	
60-18	porcelanite		3.54
60-15	porcelanite		2.99
60-13	porcelanite		3.62

*Crystallinity index derived from methods of Murata and Norman (1976).

indices which are consistent with Monterey Formation chert and porcelanite samples analyzed elsewhere (Murata and Norman, 1976). Cristobalitic porcelanite samples occur in the southwest and east portions of the study area.

Claystone and porcelanite bedding is rhythmic in character. Individual porcelanite beds are 10 cm to 13 cm thick and grade downward into shale interbeds 5 mm to 10 mm in thickness. Laminations 2 mm or less thick are common in porcelanites. Shale interbeds are siliceous, micaceous, and contain Foraminifera casts. Shale partings decrease in thickness up section. The claystone and porcelanite weather into tabular, chippy rubble and soil.

Bramlette (1946) attributed the origin of claystones, porcelanites, and chert in the Monterey Formation to a diagenetic process involving the alteration of originally diatomaceous rocks similar to those now locally present in the uppermost part of the formation. Alteration occurred after deposition through load deformation from late Miocene to early Pliocene time. Bramlette also remarked on the direct relationship of an increased depth of burial or overburden to an increase in hardness and density of porcelanite. This change in character of porcelanite is caused by a progressive alteration of amorphous opal (original diatomaceous rock) to cristobalite to quartz through an increase in temperature (Murata and Larson, 1975) which is directly related to an increase in depth of burial. Other factors of diagenesis to

be considered also are the nature of host sediment, and possible tectonic influences like folding and faulting (Murata and Randall, 1975) which may alter the original diatomaceous rock without significant overburden.

Age and Correlation. Megafossils are relatively scarce within the Hames Member and consist of specimens of Macoma sp? and small crabs. Scarce, but well preserved, fish remains also have been found. Microfossils (table 3) in thin shale interbeds indicate ages ranging from Luisian to late Mohnian from southwest to northeast, respectively.

The Hames Member as recognized here is similar to that recognized by Durham (1974) in the Salinas Valley area; both are composed predominantly of siliceous claystone, shale, porcelanite, and less common phosphoritic rocks. Durham's Hames Member is Luisian to Mohnian in age and is equivalent in age to the Hames Member as recognized here.

Depositional Environment. Microfossils from the Hames Member indicate conditions of outer neritic to upper bathyal depths during Luisian time to lower middle bathyal depths during late Mohnian time and thus indicate a deepening with decreasing age (Appendix 3). The relative scarcity, smallness, and limited variety of megafossils along with the preservation of fish remains suggest low oxygen environments (Bramlette, 1946). These conditions may be related to the oxygen minimum zone common in silled basins. The laminated character of the porcelanite and general lack of detrital

sediment suggest bathyal conditions of deposition. Bramlette (1946) remarked on the abundance of Foraminifera in unexpected and presumably inhospitable environments within the Monterey Shale, a paradox which may be explained by faunas transported from oxygenated waters to deeper, less oxygenated conditions. If one assumes that more sediment collected in the central and deeper portions of a basin relative to the edge, then the sediment thickness or overburden would be greatest in the deeper part of the basin. Based on this assumption, a highly speculative paleogeographic scheme can be derived from X-ray data shown on table 4; these suggest that the central part of the study area, indicated by quartzose porcelanites, was buried by greater amount of overburden than areas to the southwest and east parts of the study area which are characterized by cristobalitic porcelanites.

The author concludes that the Hames Member in the study area probably was deposited under deepening bathyal conditions as suggested by the foraminifers which represent slope environments with less oxygenated waters suggested by the scarcity and smallness of megafossils. Deposition may have been partly restricted as within a silled basin.

Miscellaneous Surficial Deposits

Older and younger alluvium with landslide debris of post-Miocene age unconformably overlies the Monterey

Formation. Older alluvium, consisting of river terrace deposits at different elevations, occur predominantly on the northern half of the study area and cover 15 percent of the surface area studied. Differences in elevations of these river terraces reflect a possible regional uplift of 100 m (Bowen, 1965). Terraces are composed of granitic, well rounded, boulder to cobble conglomerates set in very coarse, micaceous, arkosic matrices. These deposits have been assumed (Williams, 1970) to be no older than early Pleistocene in age.

The most recent surficial deposits consist of sand and gravel which make up the present Carmel Valley River bed, and landslide debris on the flanking hillsides. Landslide debris is composed of friable sand and shale, mostly derived from the Laureles Sandstone and the Sandholdt Member, but in part also derived from the friable portions of the Los Tularcitos Member. Landslides probably have resulted from the incompetency of source material.

TECTONICS AND STRUCTURAL EVOLUTION

The Carmel Valley area, and probably the entire West Coast, was a tectonically active area during middle Miocene time. The Robinson Fault just south of the study area was active during deposition of the Robinson Canyon Member. The Potrero Fault, also south of the study area, probably was active during early Chamisal deposition (Brown, 1962). The Tularcitos Fault appears to have been active during Chamisal deposition and may have been instrumental in production of conglomeratic material deposited in the Chamisal Formation along the fault and at the Garland Ranch Regional Park. Martin and Emery (1967) proposed a Carmel Valley Fault, extending up the valley (possibly the Tularcitos Fault?). This fault presumably originated in the early part of the middle Miocene due to initial compressional forces and subsequent tensional forces which resulted in a trough-like feature or basin framed in by relatively higher areas to the north and south. A similar paleogeographic scheme proposed by Graham (1978) shows a paleohigh area to the north, trough or basinal area in the Carmel Valley proper, and a possible shallower area farther south. The author's findings are in general agreement with both paleogeographic schemes which are typical of continental borderland topography and genesis.

The Carmel Valley area probably was a restricted or silled basin characterized by steep slopes capable of

generating fluidized or grain flows. The paleoshoreline was probably to the north as indicated by paleocurrent data, stratigraphic succession of rocks on top of granodiorite basement, and oolitic phosphate material being restricted to the north half of the study area. A deeper central trough, which may have been somewhat isolated from the open ocean by a submerged paleohigh area to the south, is suggested by X-ray data (table 4) of porcelanites, by stratigraphic thinning of units to the south, and by depth interpretations based upon benthonic Foraminifera.

Superimposed on this middle Miocene basinal configuration was folding which occurred during late Pliocene time (Williams, 1970). The present topography was derived from this folding which resulted from compressional forces probably oriented in a northeast-southwest direction. The folding is characterized by large, open, gentle folds oriented southeast to northwest in the northern part of the study area and east-west in the southern part. Differences in trend of fold axes in the southern part of the study area may have been due to obstructive paleohigh areas which affected the net directional properties of primary compressional forces on yielding strata.

Faulting resumed during late Pliocene to earliest Pleistocene time (Williams, 1970). Faults apparently do not offset the older alluvium of Pleistocene age. The southeast-to northwest-oriented Berwick Canyon and Snivleys faults were

formed during this time, and there was a resumption of movement along the Tularcitos Fault. The Tularcitos Fault may connect with the Berwick Canyon Fault (Thorup, 1976), head out to sea toward the Carmel Bay submarine canyon (Bowen, 1965), or connect with the Navy Fault north of Carmel Valley and continue under the Monterey Bay (Clark and others, 1974). Faults concealed beneath the Carmel Valley alluvium have been recognized on the basis of gravity studies done by Sieck (1964). The faults are probably high angle and normal. It is postulated that right-lateral strike-slip movement has taken place on the Tularcitos Fault (Bowen, 1965; Graham, 1976) because similar facies apparently are offset along the fault.

PHOSPHORITIC ROCKS

Nomenclature

"Phosphate rock" is a term applied to any rock containing more than 20 percent P_2O_5 . "Phosphorite" is a genetic term referring to phosphate rock which originated in a marine environment (Cathcart and Gulbrandsen, 1973). By these standards, the marine rocks of the Robinson Canyon-Laurles Grade area, which contain less than 20 percent P_2O_5 , are neither phosphate rock nor phosphorite. These rocks are more appropriately called phosphoritic rocks.

Phosphate occurs in a variety of forms within the phosphoritic rocks. These forms are identical to some textures in limestones; thus, the morphological basis which Folk (1974) used in his classification of limestone constituents has been adopted for the classification of the Carmel Valley phosphoritic rocks. The phosphate is contained in a microcrystalline matrix material like micrite, in a colored translucent to transparent cement-like sparite, and in allochemical constituents like oolites, pellets, intraclasts, and bioclasts. The more common constituents in the Carmel Valley phosphoritic rocks are the allochemical constituents. An additional and common category of allochemicals called non-centered pellets, also is present. Different phosphoritic forms dominate at different localities in the Carmel

Valley; thus, Galliher's (1931) description of phosphoritic oolitic rocks (actual locality not found, but mentioned to be 25 km from Carmel) and Roger's (1944) report of phosphoritic pelletal rocks at localities Mf-R-1 (T33-1) and Mf-R-2 (T332-9) apparently both are accurate.

Stratigraphic Occurrence and Bedding Characteristics

Phosphoritic beds in the Carmel Valley occur as silty to sandy beds similar in bedding characteristics to sandstone interbeds within the Sandholdt Member (fig. 7). These phosphoritic beds have a greater area distribution than the sandstone interbeds, occurring throughout the study area. Despite such a vast areal spread, phosphoritic beds are fairly restricted vertically. These beds normally occur at the contact between the Sandholdt and Hames Members or within the basal portion of the Hames Member.

Phosphoritic beds generally are 3 to 10 cm thick, but they may be as thick as 25 cm. These beds have a fresh color of medium light gray (N6) and a weathered color of light brown (5YR5/6). Phosphoritic beds commonly show normal grading as indicated by concentrations of pelletal and oolitic phosphate with pebbles of phosphate in the basal portion. The upper portion of individual phosphoritic beds grades into overlying siltstone and shale, but where beds are encompassed by porcelanite in the Hames Member, contacts are fairly sharp. Basal contacts of all phosphoritic beds



Figure 7. Phosphoritic bed with light brown limestone concretions at measured section 191 (top of hammer is the base of bed).

are distinct, many showing load features, flame structures, convolute laminations, filled pockets, and development of pseudo-nodules (figs. 8 and 9). Normally the underlying material is much finer grained than overlying phosphoritic material. Water escape structures were recognized in thick beds with phosphoritic pebbles suspended in matrix (fig. 10). Matrix material in phosphoritic beds is composed of microcrystalline quartz, cristobalite, and clay minerals. It averages 45 percent, but may be as high as 72 percent. Burrow structures of possibly the Chondrites-Nereites assemblages occur in one thick phosphoritic bed. Phosphoritic beds are fairly resistant relative to encompassing lithologies except when interbedded within harder porcelanites.

Unusual phosphoritic beds 5 cm to 10 cm thick occur higher in the lower portion of the Hames Member. They are exposed as resistant series of parallel beds projecting above the ground surface (fig. 11). These phosphoritic rocks resemble pebbly conglomerates and consist of 5-mm to 10-mm, semi-rounded to angular, phosphoritic clasts in a clayey to sandy matrix. Much of the phosphatic material has been leached. Float material from these beds occurs throughout the central portion of the study area.

The characteristics of beds associated with the phosphoritic rock sequences suggest rapid deposition of the phosphoritic rocks over soft, semi-consolidated sediment. Phosphoritic beds probably were deposited from fluidized flows



Figure 8. Convoluted bedding, load cast features, and pebbles of phosphate in a phosphoritic bed (locality at measured section 332).



Figure 9. Load casts with pellets and pebbles of phosphate in a phosphoritic bed (locality at M-Y-334).

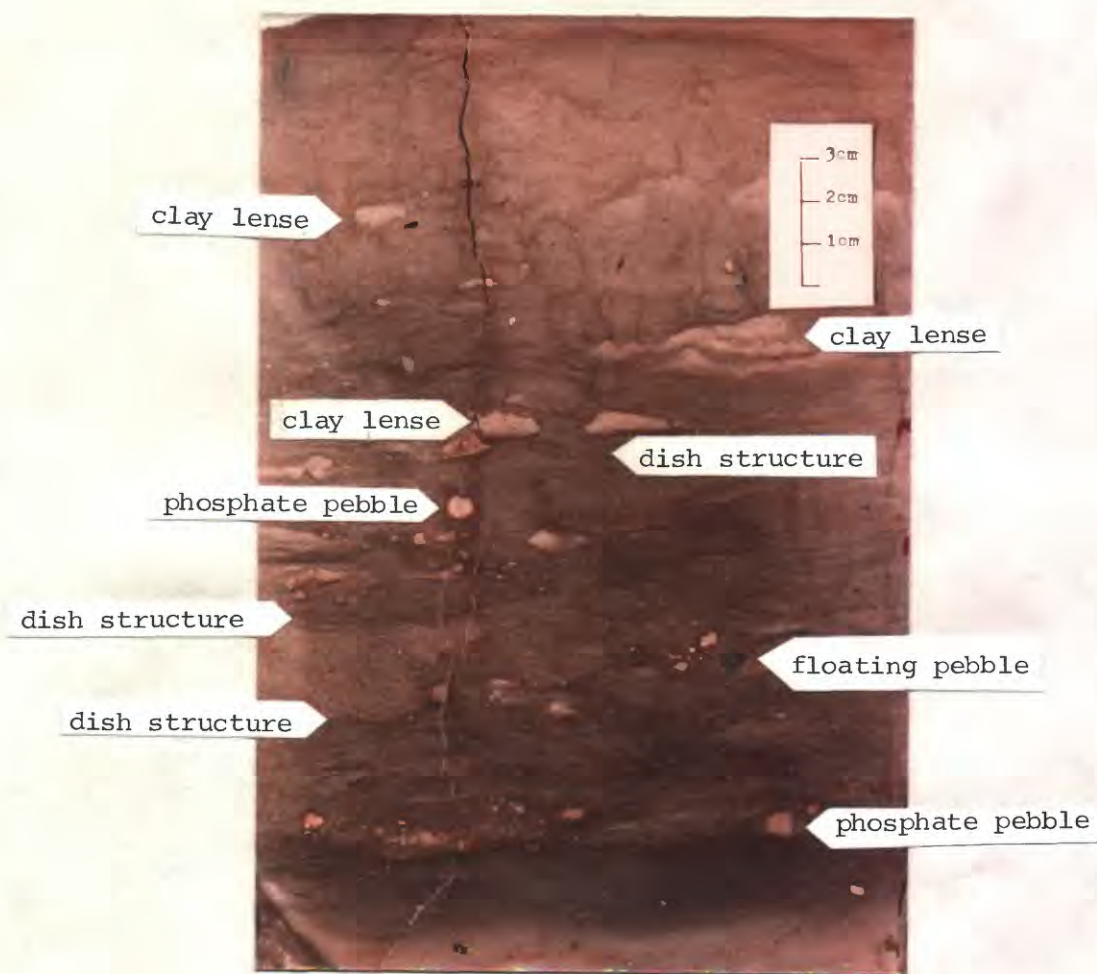


Figure 10. Possible water escape structures in a thick phosphoritic bed (locality at measured section 332).



Figure 11. Resistant phosphoritic beds in the basal portion of the Hames Member (locality just south of T316).

and possibly represent turbidites subsequently modified through liquefaction and fluidization. Phosphoritic beds stratigraphically higher in the Hames Member have characteristics consistent with that of debris flows.

Petrography

Oolites

Oolites, which occur only north of the Carmel River within the study area, are present in the phosphoritic rock in amounts ranging from zero to 27 percent (table 5). No rock was found in which all the phosphate is in oolites; the highest percentage is 60. The oolites generally are mixed with other phosphate constituents, most commonly pellets.

In the oolite-dominated rocks the oolites range from 0.2 mm by 0.3 mm to 0.35 mm by 0.4 mm in size. Oolites are fairly well sorted and are spherical to ellipsoidal in shape. Surficial color ranges from a darker hue of pale brown (5YR-5/2) to lighter hues of pale red (10YR6/2) and grayish-orange-pink (10YR8/2). Gradations of color are probably a function of oxidation (bleaching) due to weathering, although there is a possibility that surficial colors may reflect depositional environmental conditions just prior to burial. The presence of iron oxides and organic material may affect coloration.

Internal concentric rings, differentiated by alternating colors of light and dark hues, are common in these oolites. Alternating colors may be a function of the concentration of organic debris, oxidation, or iron oxide content. Such

rings also may reflect changing environmental conditions during oolite formation. Rings are both uniform and non-uniform in thickness. Some rings show areas of thickening and thinning, but individual rings are fairly homogeneous in color. Some oolites contain no rings, but others have as many as six (fig. 12). All rings, despite coloration, are isotropic under polarized light. Some oolites have siliceous rims; these rims may produce the semi-polished surfaces common on pellets and oolites. Boundaries of oolites are sharp, well defined, and smooth. Included detrital grains near the oolite rims generally are conformable with the rim boundary and do not protrude through it.

A detrital grain centrally located or off-center is present in most oolites. This grain commonly is monocrystalline, nonundulatory quartz, plagioclase, or K-spar, and less frequently a complete diatom, black carbonaceous debris, or phosphatic organic debris (fish scale, bone). These grains show partial to almost complete replacement by phosphate. Grains range from 0.1 mm to 0.2 mm in diameter and are equant and fairly angular. Differences between included detrital grains and surrounding exterior framework grains are very subtle. Included grains may or may not be similar in size and angularity to exterior framework grains. Some included grains are slightly larger than exterior counterparts, and others show a higher proportion of plagioclase grains. The size of the included



Figure 12. Oolite (T334-1) in white light showing at least five generations of growth indicated by light and dark brown rings.

grain compared to overall oolite-size ratio ranges from one third of the entire oolite (large oolite) to almost equivalent in size (small oolite) with a very thin phosphate rim encompassing the grain. This difference probably is due to different stages of phosphate addition to the included grain.

The phosphate contained within the oolite is cryptocrystalline, isotropic, and is called collophane (Dietz and others, 1942). The collophane contains abundant diatom debris and clay minerals. Oolites commonly display a concentric orientation of included clay laths (fig. 13). Included detrital grains also show a preferred concentric orientation in a few samples (fig. 14). Although the concentric orientation of included clay minerals could be related to recrystallization, orientation of included detrital grains would seem to rule out this possibility. In addition, muscovite-illite laths within the matrix show no preferred orientation or subsequent recrystallization, thus, an accretionary process of phosphate addition possibly through rolling motion is indicated. One sample indicates recrystallization of collophane into francolite. In this particular sample oolites under polarized light have distinctive black crosses which probably result from development of true fibroradiated spherulites (Carozzi, 1960). Porcelanites within the Hames Member show effects of overburden as indicated in their quartzose mineralogy; thus, some oolites which exhibit black crosses under polarized light may have been recrystallized promoted by deep burial.

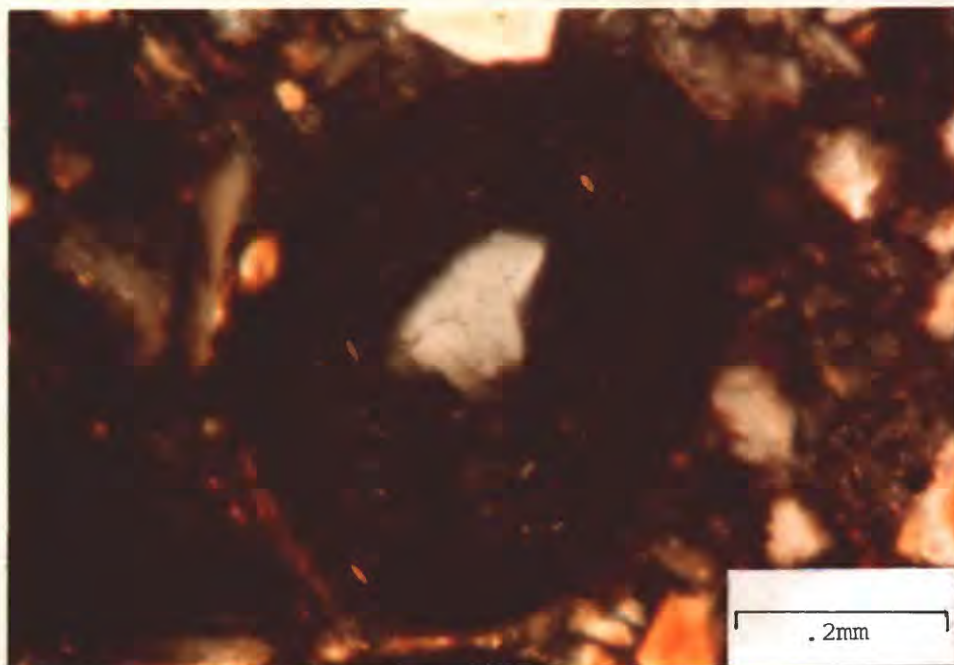


Figure 13. Oolite (T176) in polarized light showing concentrically oriented muscovite-illite laths.

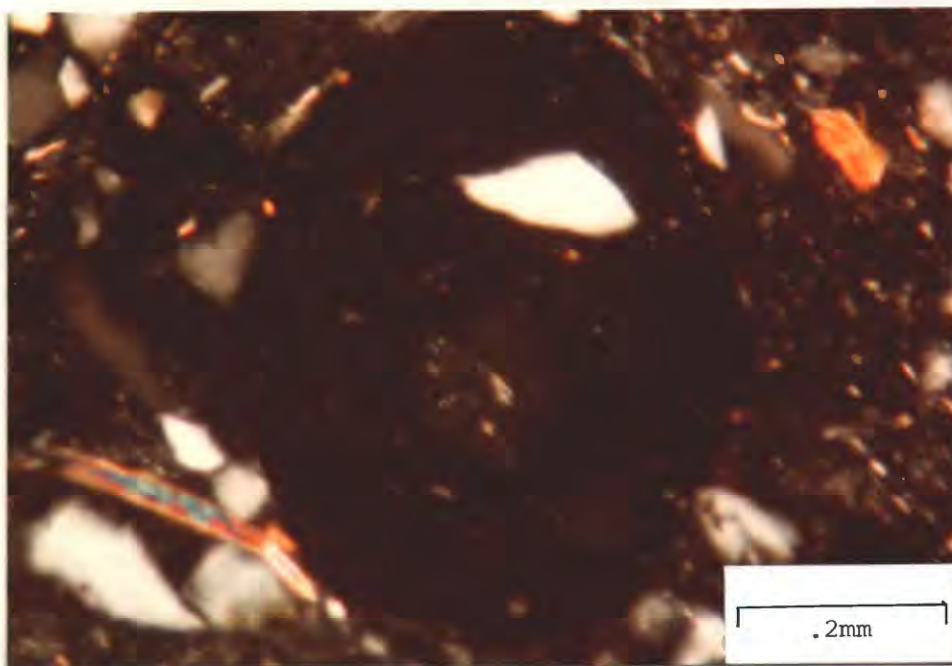


Figure 14. Oolite (T176) in polarized light showing possible oriented quartz detrital grain (other than nuclei).

Phosphoritic oolites cannot be shown to be replacements of calcareous oolites. In addition, no calcite occurs either as matrix or cement in oolite-dominated samples. The only replacement of phosphate material is by silica, notably on the rims of oolites.

The matrix and other framework constituents in oolite-dominated rocks are very similar to those in phosphoritic rocks composed of non-oolitic-dominated constituents. There are subtle differences, however. Oolitic rocks may or may not be framework-supported, and oolites may or may not be in contact with each other. Detrital grains are composed predominantly of monocrystalline, non-undulatory quartz and feldspar. Present, but less common, are broken oolites, biotite, organic debris, and glauconite. The matrix generally is composed of clay minerals and other clay-sized material, and averages 44 percent of the rock. Iron oxides are fairly common as cement material and are disbursed within the matrix in amounts up to 9 percent.

Overall, oolites indicate formation by mechanical accretion as shown by oriented clay laths and included detrital grains. Coloration of concentric rings possibly indicates variable environmental conditions during oolite formation, which may have resulted from changes in oxygen content brought about by organic activity or fluctuations

in sea level. Burial diagenesis may have caused some oolites to be recrystallized as indicated by radial orientation of phosphatic material, but the majority of oolites show no indication of recrystallization.

Pellets

Pellets occur throughout the study area and with both oolites and non-centered pellets. Pellets are present in phosphoritic rocks in amounts of 3 to 45 percent.

Pellets are larger than oolites, ranging from 0.1 mm by 0.2 mm to 0.5 mm by 0.7 mm with some as long as 1 mm. Pellets in any one sample are more or less uniform in size. Pellets generally are elongate, ellipsoidal, oblate, less commonly spherical, and in some samples very irregular in shape. Elongated pellets may or may not be oriented parallel to bedding. In matrix-supported samples elongated pellets tend to lack orientation, whereas in framework-supported samples elongated pellets show weak orientation parallel to bedding.

Surficial and interior coloration are the same and range from very light varieties of grayish-orange-pink (10R8/2) to darker varieties of pale brown (5YR5/2). The lightest colored phosphate-bearing constituents are pellets. Color variations probably are due to the same conditions which affected oolite coloration.

Pellets have no rings and show no preferred orientation of included material. Internally, the pellets are

massive, but some samples exhibit a faint grapestone structure or crude mosaic pattern (fig. 15). Some pellets have siliceous rims similar to those around oolites. Pellets generally have distinct boundaries, although some have very fuzzy boundaries (fig. 16). These less distinct pellets contain detrital grains piercing the pelletal rim and approach the condition of non-centered pellets. Fuzzy boundaries of pellets could have been caused by leaching of phosphate material, but several characteristics of fuzzy, bounded pellets do not support such an interpretation. A uniform coloration extends throughout the fuzzy pellets rather than being a gradational or semi-zoned coloration expected from a leaching process. Also, collophane occurs only within the fuzzy pellet rather than in both pellet and encompassing matrix as would be expected if phosphate material had been leached out of the pellet. Arguments against leaching and the encompassing of detrital grains along the perimeter of fuzzy pellets more strongly indicate a process of in situ concretionary growth of phosphatic material for fuzzy pellets.

Pellets generally are composed of collophane and included clay minerals and in some cases abundant diatom debris (fig. 17). Inclusion of complete diatoms is not uncommon (fig. 18). Diatoms found included in Carmel Valley pellets previously collected by Rogers (1944) and identified by G. Dallas Hanna are listed on table 3.

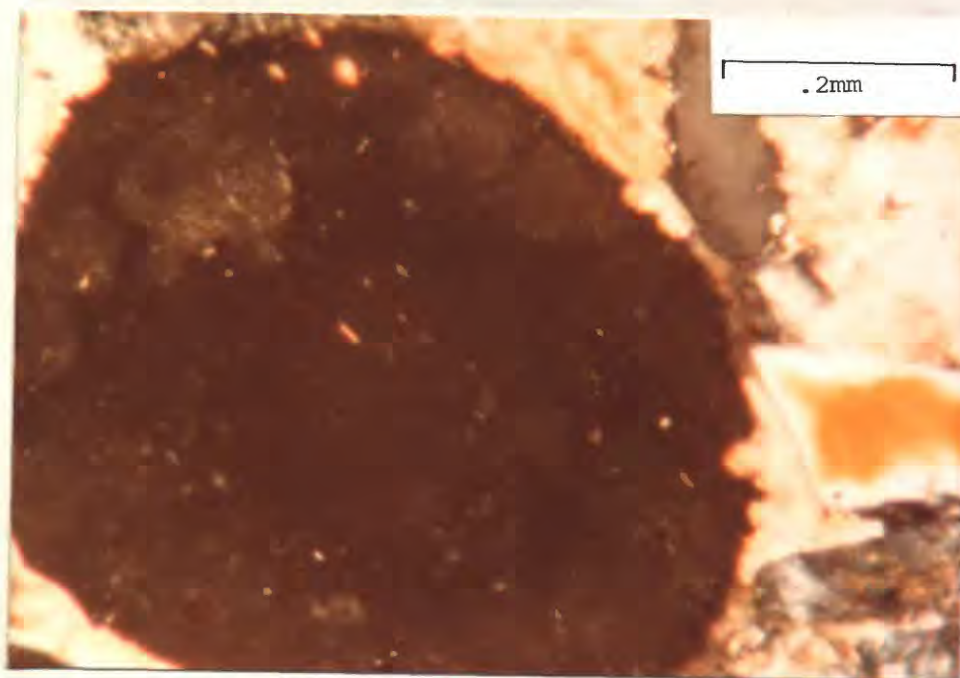


Figure 15. Pellet (T399-6) in white light showing grapestone or crude mosaic structure.

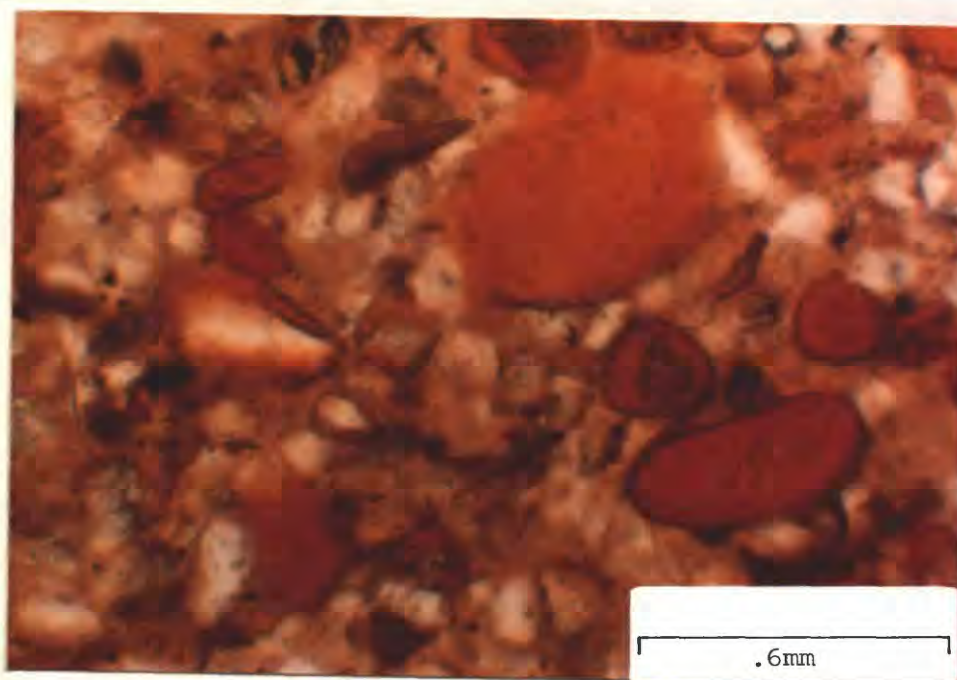


Figure 16. Fuzzy pellet (T332-7) in white light with other pellets of various sizes.

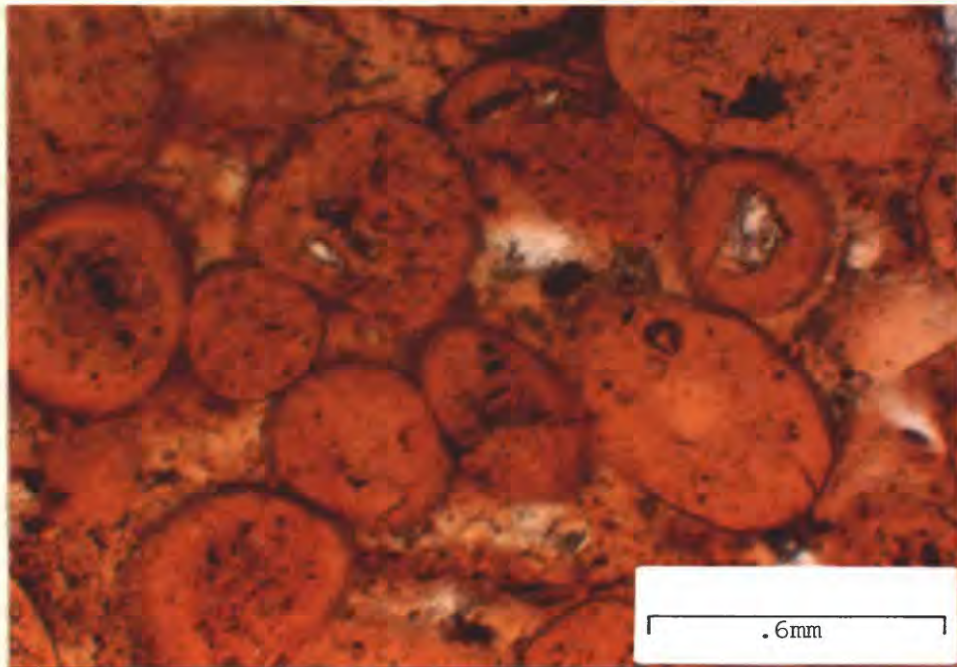


Figure 17. Pellets (T332-14) in white light showing included diatom debris (dark material).

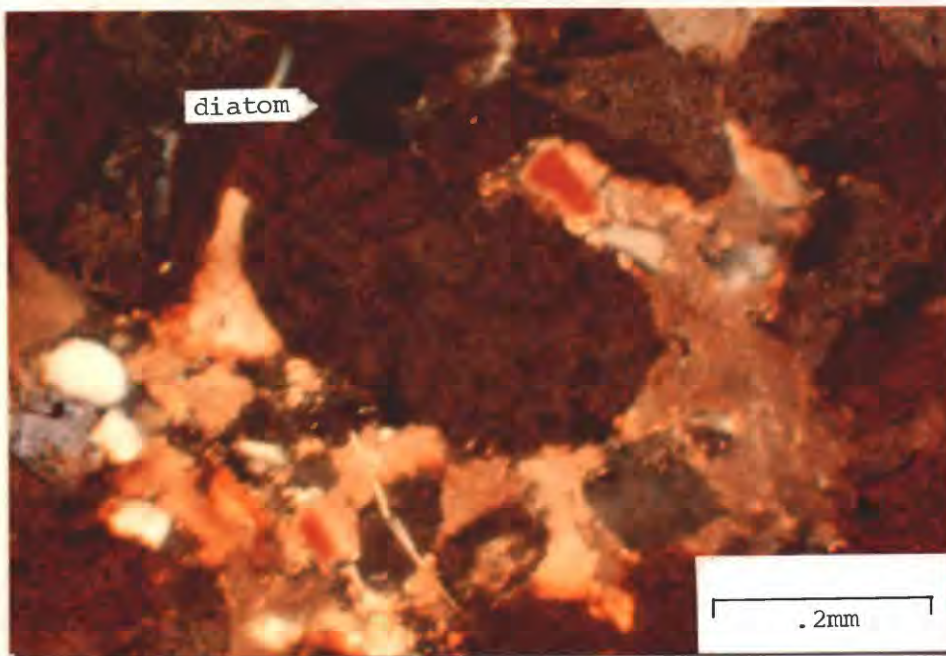


Figure 18. Pellet (T332-14) in white light showing a complete diatom included.

Pellets commonly contain no detrital quartz or feldspar grains. In some samples material in the interior of the pellets looks finer than that in the matrix, but in others it appears identical. Pellets tend to have fewer illite laths than oolite.

No pellets contain remnant calcium carbonate or any indication calcium carbonate has been replaced by phosphate. In fact, a common feature is that in which calcite has replaced phosphate through embayed contacts, notably at the rims of pellets embedded in calcareous matrices. Calcareous sparite also occurs as vein fillings in cracked pellets. Silica commonly has replaced both calcite and phosphate. The mosaic pattern in some pellets may be caused by some replacement process.

Pelletal rocks may or may not be framework-supported. Non-pelletal framework constituents are similar to those in oolitic phosphoritic rocks; however, more angular phosphate fragments, organic debris, calcite-filled foraminifers, twinned plagioclase, lithic fragments (granitic and schistose clasts), and biotite are present in pelletal rocks than in oolitic rocks.

The matrix in pelletal rocks is more abundant than in oolitic rocks and averages 50 percent. Most commonly the matrix is clay, but there also are calcareous matrices, and less frequently and in considerably smaller patches, collophane. One sample (T259-3) exhibited phosphoritic

pellets encompassed in calcareous sparite and shelly debris. No material in this sample exhibited indications of being phosphatized; the only replacement minerals noted were calcite which had replaced rims of pellets and silica which had replaced shelly debris and patches of micrite matrix. Cementing agents range up to 13 percent in pelletal rocks and include calcareous sparite, collophane, and lesser amounts of iron oxides.

Non-centered Pellets

The non-centered pelletal category introduced by the author includes pelletal phosphate with grain inclusion(s) which are not oolites. This phosphate constituent constitutes up to 10 percent of the total rock and may account for 40 percent of the total phosphate constituents in some rocks. At only one locality (T379) are the non-centered pellets the dominant phosphate constituent. Despite this lesser abundance, non-centered pellets occur commonly with pellets, less commonly with oolites, and throughout the study area.

Dimensions and shapes of non-centered pellets are variable and comparable to that for pellets. Non-centered pellets normally are poorly sorted. Surficial and interior coloration, lack of included circum-oriented material, and boundary definitions ranging from distinct to vague, are all characteristics common to non-centered pellets and pellets.

Non-centered pellets, however, are characterized by detrital grain inclusions of quartz and feldspar.

Non-centered pellets may contain one or more detrital grains which may or may not be centered. Those with centered grain inclusions are similar to oolites, but lack colored zonation or rings and concentrically oriented illite laths. Grain inclusions more commonly are off-centered. Included grains are composed of monocrystalline, non-undulatory quartz, feldspar, and chert. Grains range in size from 0.1 mm to 0.15 mm and are equant and angular. In non-centered pellets with a single included grain, the grain to pellet size ratio may range from 30 percent to as high as 90 percent. Under polarized light, grain inclusions are indistinguishable from surrounding framework grains other than being encompassed in isotropic collophane material (figs. 19 and 20). Many included grains protrude out from non-centered pelletal rims (figs. 21 and 22).

Framework material, matrix, and cement are similar to those in pellets as are the textures. Samples with significant amounts of non-centered pellets commonly contain bioclastic material such as fish scales and microscopic bones.

Intraclasts

Phosphatic intraclasts are fairly common and are the predominant constituent in phosphoritic beds in the basal portion of the Hames Member. Phosphoritic materials other

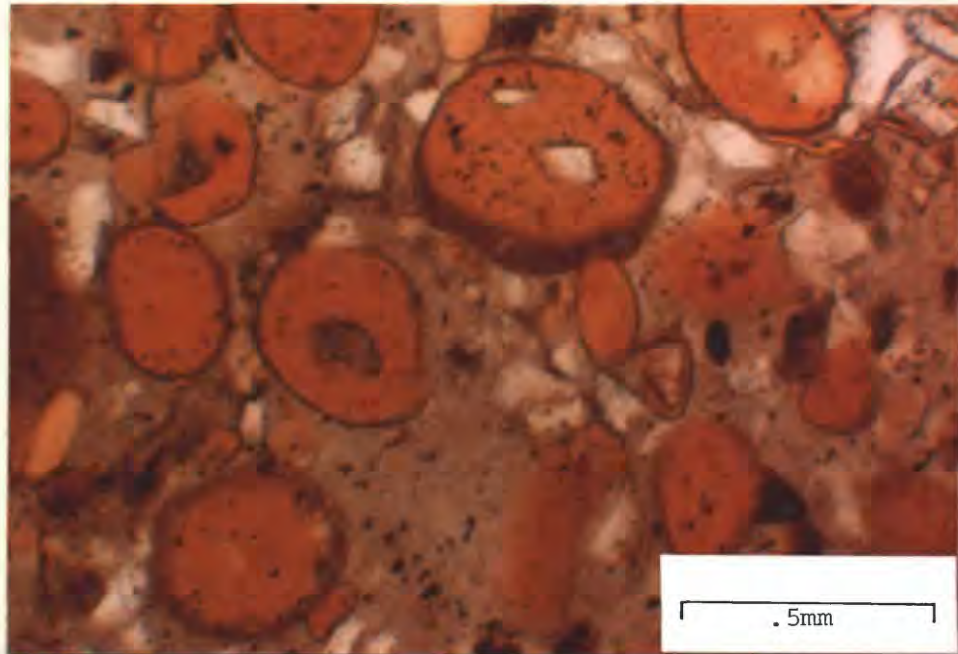


Figure 19. Non-centered pellets (T96-5) in white light.

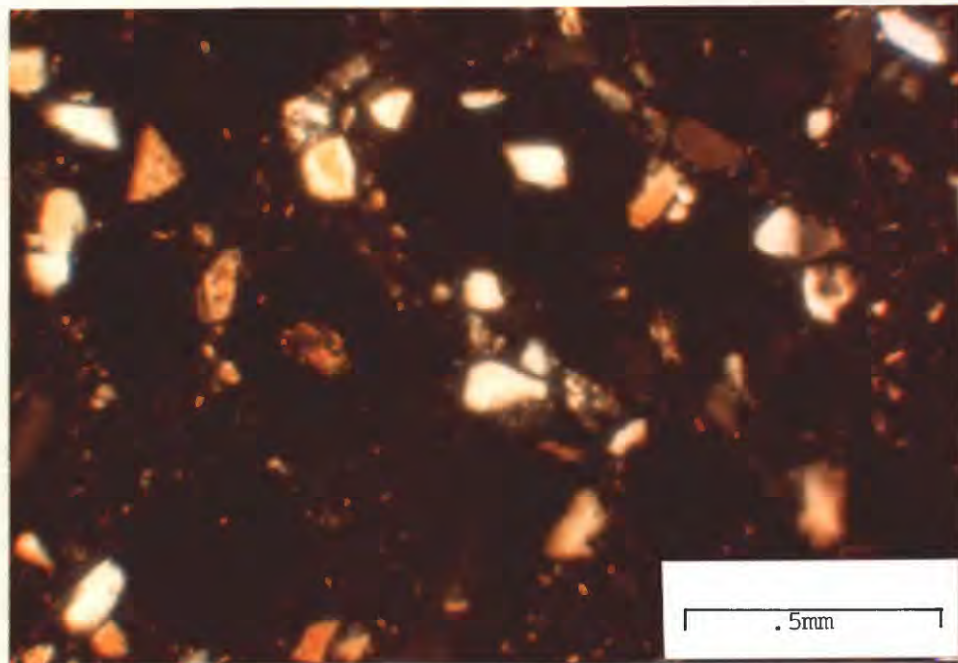


Figure 20. Same as figure 19, but in polarized light to emphasize the similarity in size and shape of included grains and framework grains.

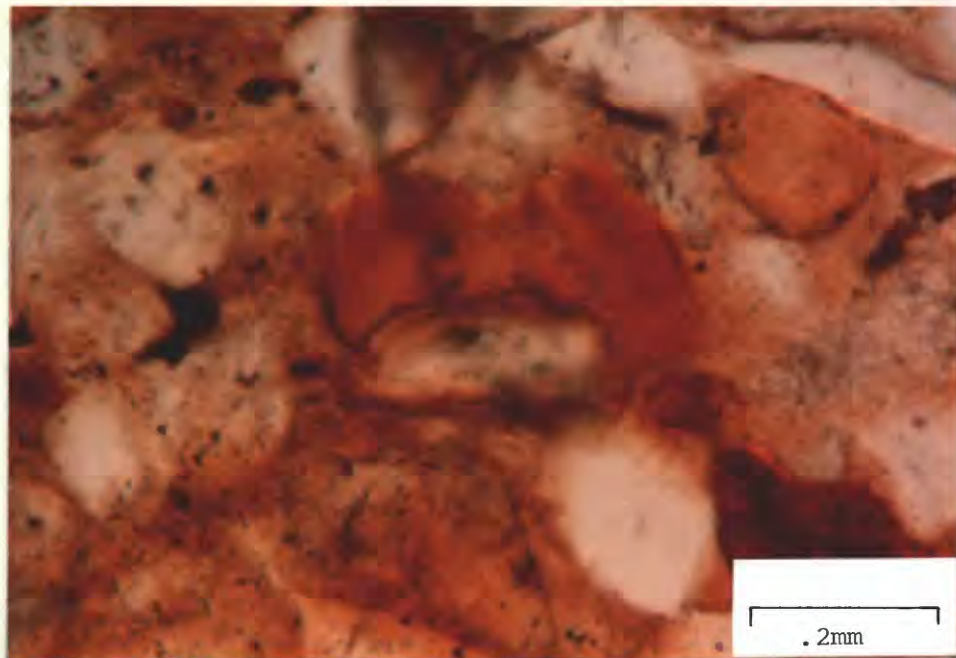


Figure 21. Non-centered pellet (T96-5) in white light showing both protruding and intruding grains.

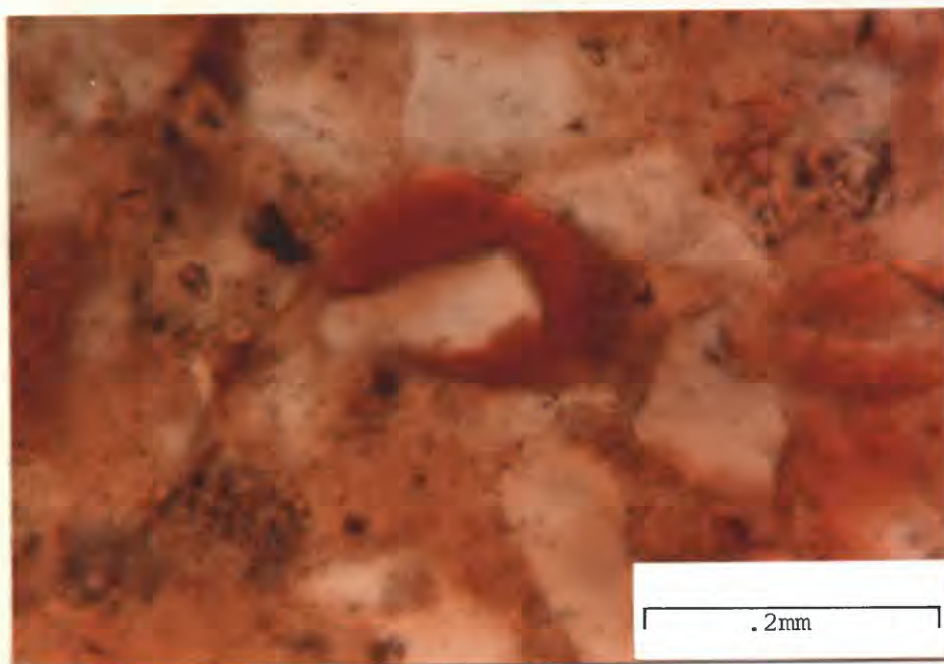


Figure 22. Non-centered pellet (T332-7) in white light showing a protruding detrital grain.

than bioclasts which are larger than pelletal material and do not have an overall pelletal shape are considered intraclasts. Such intraclasts may be as large as 1.5 cm. They normally are irregular in shape, angular to subrounded, and tend to be a very pale orange (10YR8/2), a lighter color than pellets and oolites.

Intraclasts may be composed of cemented pellets and oolites or massive phosphoritic material. The density of grain inclusions in intraclasts is variable, but never as great as that in the surrounding material. These phosphoritic pebbles probably were eroded from bedded phosphates or they may represent pseudo-nodules (Blatt and others, 1972) which were set free by the erosive actions of bottom or turbidity currents.

Bioclasts

Bioclasts in phosphoritic rocks are minor constituents in the form of fish scales, and large and small bone debris. Phosphatic bioclasts are common in shale beds in the Sandholdt Member which contain abundant foraminifers.

Geochemistry

Previous chemical analyses have been made of the Carmel Valley phosphoritic rocks by Rogers (1944) from localities Mf-R-1 (T333-1) and Mf-R-2 (T332-9). Pellets placed in hot dilute nitric acid left an insoluble residue which amounted

to approximately 5 percent of the original pellet weight. Chemical analysis of individual pellets showed that they were 33.11 percent P_2O_5 and contained large amounts of calcium, moderate amounts of aluminum, no appreciable iron, and a small amount of magnesium. The overall composition of the pellets was determined to be collophane by Rogers (1944).

Chemical analyses of the Carmel Valley pelletal and oolitic phosphoritic rocks show a range of 3.4 to 16 percent P_2O_5 content. Sandstones from the Tularcitos Member and Laureles Sandstone, at localities C60-1 and C276-1 respectively, also show small amounts of P_2O_5 which petrographically shows up as cement. Analyses of the Carmel Valley phosphoritic rocks are shown on table 6.

Petrographically, pelletal and oolitic phosphoritic rocks of samples geochemically analyzed indicated collophane content ranging from 13 percent to 61 percent (table 5). If one assumes that all P_2O_5 is contained in collophane ($Ca_{10}[PO_4CO_3]F_{2-3}$) (Altchuler and others, 1958), then P_2O_5 content should be approximately 31 percent of the total collophane content. Figure 23 indicates, however, that the majority of samples are impoverished in P_2O_5 , although some samples, notably 108 which contains a significant amount of collophane cement petrographically, are enriched. Figure 23 also indicates a trend for oolitic rocks to be slightly more phosphatic than pelletal rocks. Pelletal rocks appear to

Table 6. Semiquantitative analyses of phosphoritic rocks from the Robinson Canyon-Laureles Grade area.

WEIGHT PERCENT OXIDES	C467-1 Tct	C467-2 Tct	C457 Tct	C60-1 Tct	C276-1 Tml	C259-1 Tml	C423-1 Tml	C259-2 Tml	C60-8 Tms	C332-15Tms	C332-19Tms	C191-4 Tms	C259-3 Tms	C60-14 Tms	C62 Tms	C99 Tms	C108 Tms	C137 Tms	C176 Tms	C332-13Tms	C371 Tms	C380 Tms	C191-7 Tms	C393 Tms	C436 Tms	C461 Tms	C41 Tms	
P ₂ O ₅	<.16	<.16	<.16	2.3	1.6	<.16	<.16	<.16	.5	<.3	<.3	3.4	3.4	4.6	3.4	6.9	11.5	11.5	16	4.6	11.5	11.5	3.2	16.0	>11	3.7	3.9	
Fe ₂ O ₃	1.1	1.9	.92	1.0	1.4	.99	.54	.74	1.4	1.4	1.4	7.3	.7	1.4	2.8	1.4	2.1	2.1	1.5	1.4	2.8	1.5	2.7	1.4	2.3	1.7	2.4	
MgO	.38	.55	1.3	.1	.5	.60	.27	.81	.5	.8	.8	.56	.8	.3	.3	.1	.2	.2	.2	.1	.5	.2	.2	.2	.25	.30	.3	
CaO	2.7	15	24	2.1	.7	1.5	6.3	>27	4.2	1.4	4.2	9.4	>14	4.2	1.4	4.2	7	4.2	7	7	7	9.8	4.8	7	2.4	3.4	3.2	
TiO ₂	.3	.12	.15	.2	.5	.15	.05	.067	.3	.3	.3	.16	.1	.2	.8	.1	.2	.1	.1	.1	.3	.2	.1	.3	.2	.07	.20	.25
SiO ₂	>73	>39	>24	>21	>21	>73	>73	24	>21	>21	>21	>73	3.2	>21	>21	>21	>21	>21	>21	>21	>21	>21	>73	>15	>30	>56	>73	
Al ₂ O ₃	10	7.4	4.0	9.5	9.5	8.5	7.6	3.6	9.5	5.7	5.7	4.2	1.3	3.8	5.7	1.9	2.8	.9	1.3	1.3	3.8	2.8	1.9	9.1	3.8	6.8	4.2	5.3
Na ₂ O	2.0	1.5	1.4	2.0	2.0	2.0	2.3	1.3	.7	.9	.9	.3	.2	.3	.4	.9	1.4	.9	.4	.9	.9	.9	.9	.4	.18	.57	.65	
K ₂ O	2.4	1.9	1.8	3.6	2.4	3.1	4.6	1.7	1.2	1.2	1.2	1.0	.2	.8	1.2	.8	1.2	.6	.6	.8	.8	.6	2.1	.6	.34	1.5	1.5	
MnO	.032	.09	.95			.018	.032	.067				.21											.025		.01	.01	.01	

Tcr-Robinson Canyon Member (Chamisal Formation)
 Tct-Los Tularcitos Member (Chamisal Formation)
 Tml-Laureles Sandstone Member (Monterey Formation)
 Tms-Sandholdt Member (Monterey Formation)
 Tmh-Hames Member (Monterey Formation)

%P₂O₅ = 31% collophane line

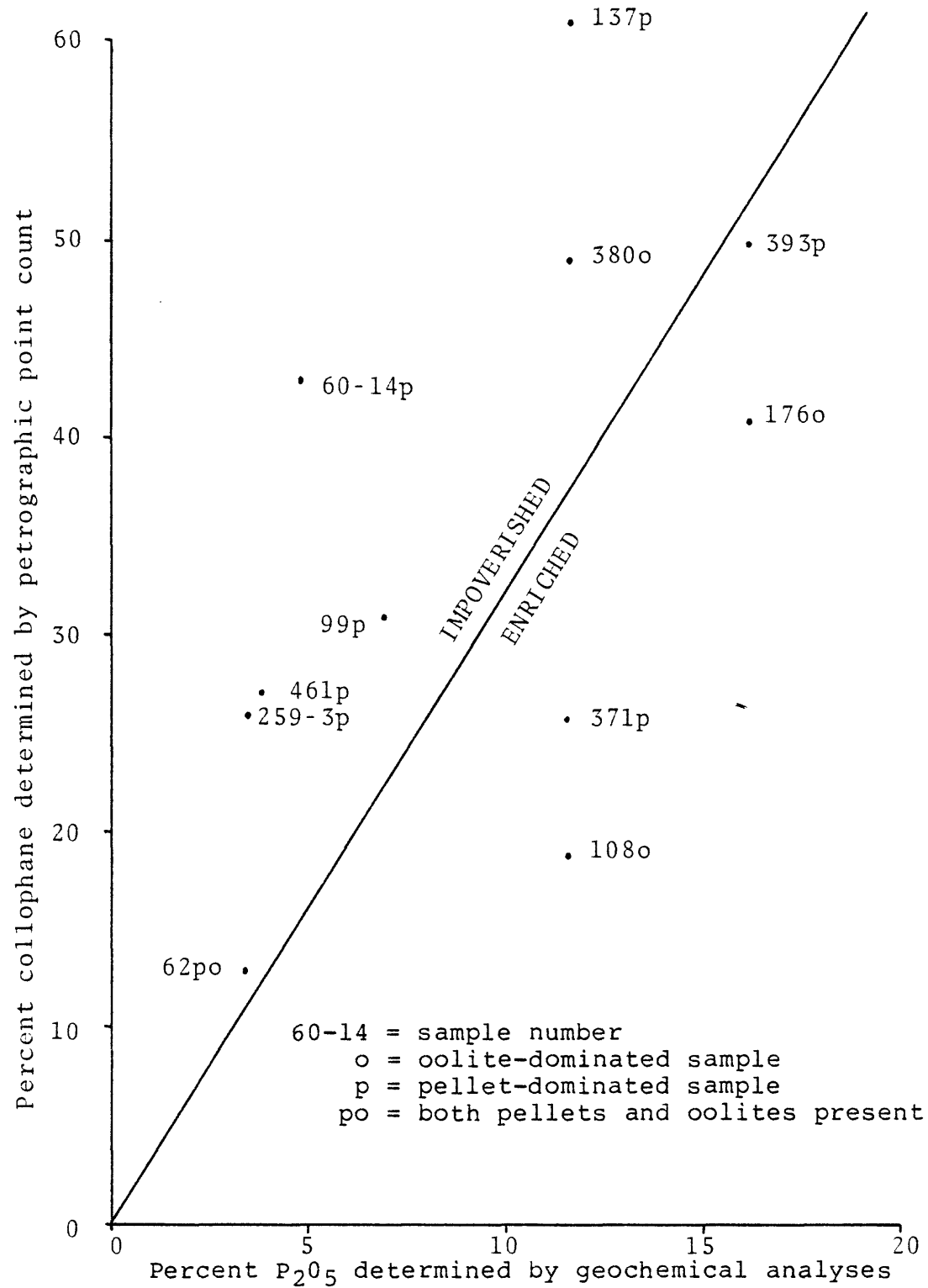


Figure 23. Plot of collophane determined petrographically with respect to P₂O₅ content determined through geochemical analyses

have the widest scatter of P_2O_5 content with respect to the ideal percent $P_2O_5=31$ percent collophane line. These differences of P_2O_5 content are the results of different origins of pellets and oolites and subsequent diagenesis which are more thoroughly explained (hypothesized) under the section "Origins of Phosphoritic Rocks and Conclusions."

X-ray Analysis

Only pelletal and oolitic collophane material was X-rayed in the phosphoritic rocks. Diffraction patterns show that the collophane material is predominantly composed of carbonate-fluorapatite. Oolitic-dominated and pelletal-dominated collophane differ in composition as expected (figs. 24 and 25).

Oolitic material (X176) contains considerably more quartz and feldspar than the pelletal material as indicated on X-ray diffraction patterns; quartz and feldspar content probably are due to grain inclusion(s). All quartz may not be due to detrital inclusion(s); some may be due to diagenesis of opaline material as shown in previous chert and porcelanite samples (table 4). The X-ray diffraction peak of quartz at 2θ equals 67.74° was not strong enough to indicate whether the quartz content is primarily due to included quartz or possible diagenesis of opaline material. A kaolinite peak is detected in X176. Kaolinite commonly is formed by the alteration of alkali feldspars in an acid

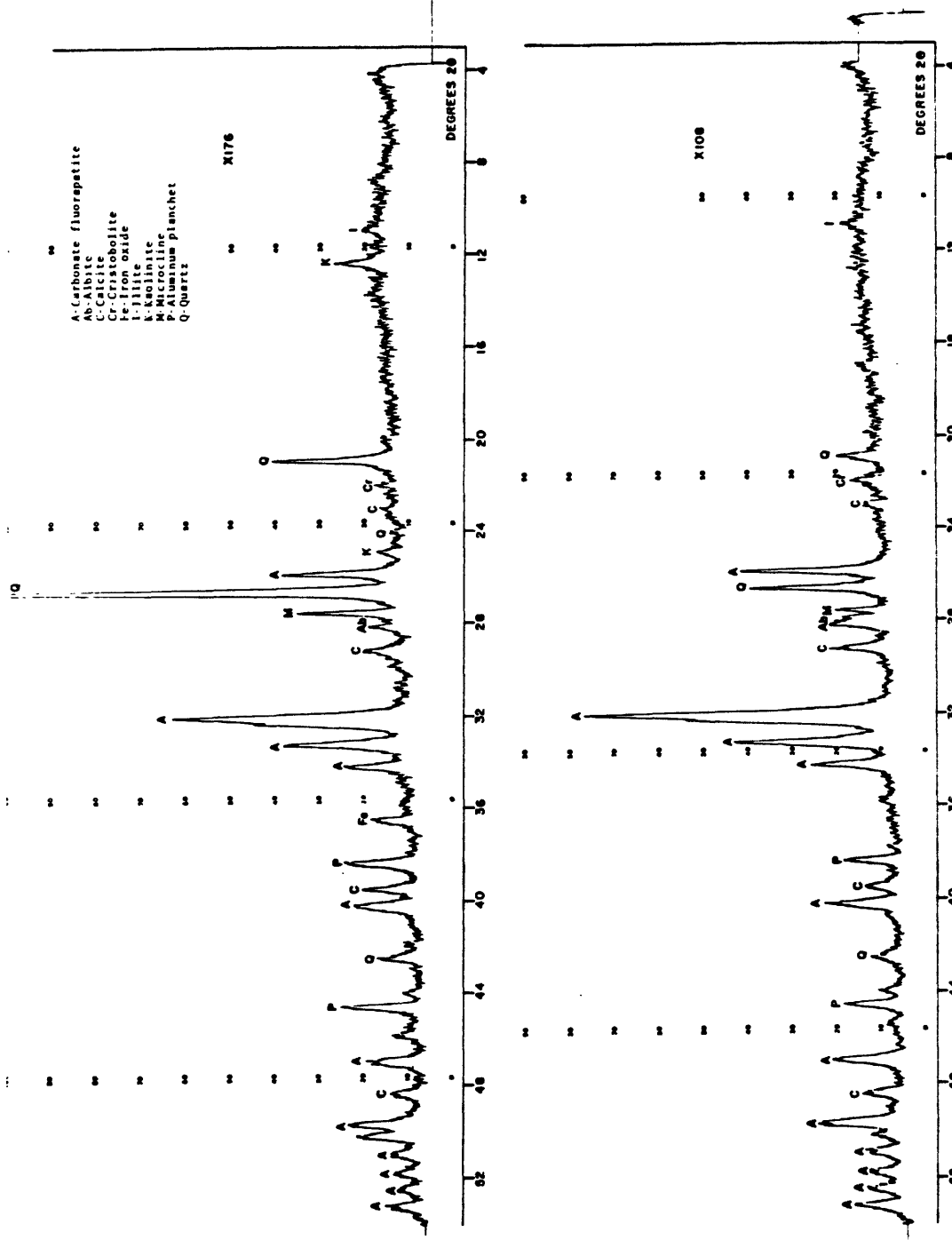


Figure 24. X-ray diffraction patterns of oolite-dominated samples using nickel-filtered copper $K\alpha$ radiation at a scan rate of one degree 2θ per minute.

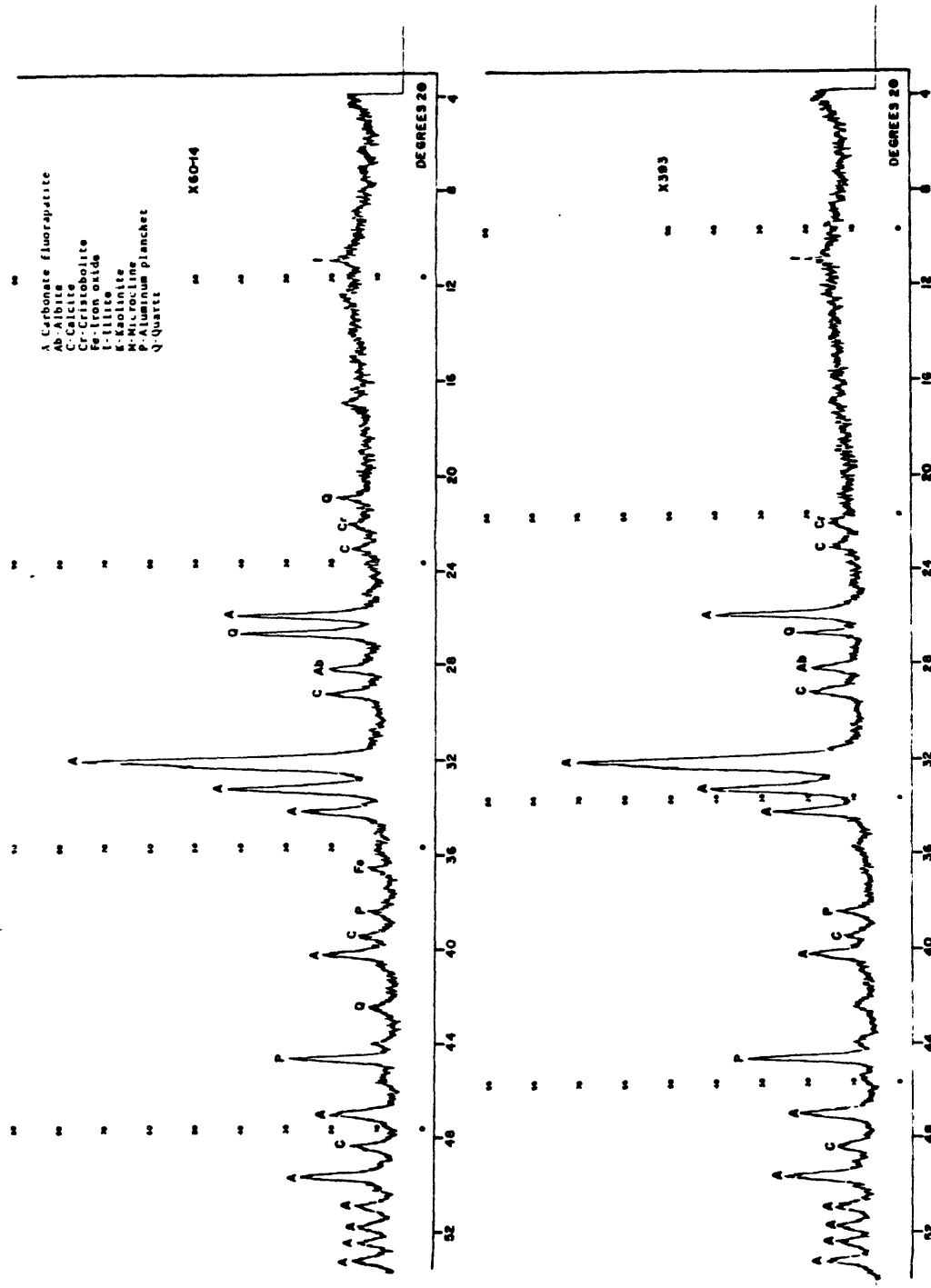


Figure 25. X-ray diffraction patterns of pellet-dominated samples using nickel-filtered copper K α radiation at a scan rate of one degree 2 θ per minute.

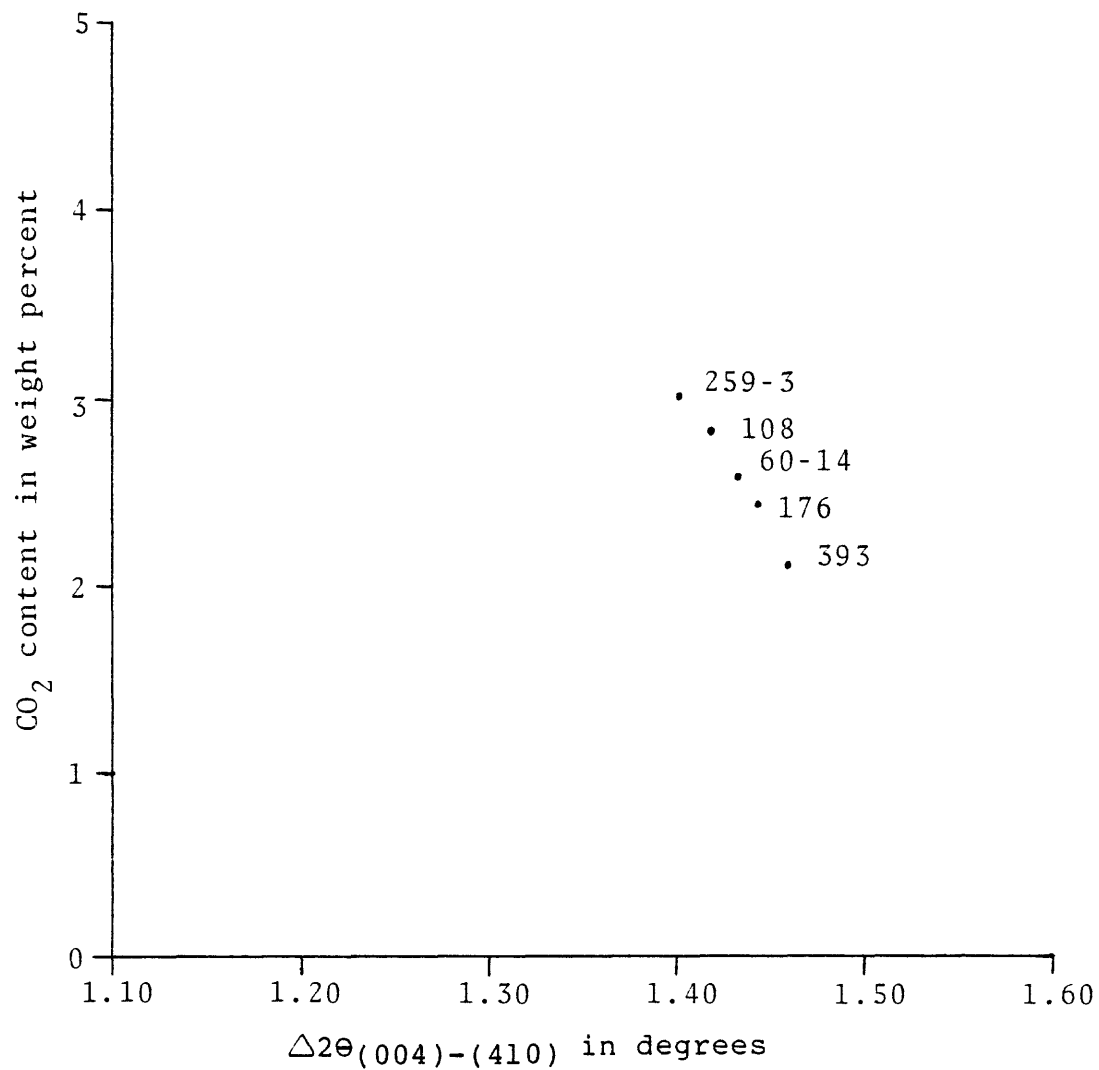
environment (Mason, 1966). High feldspar content may be the source for the kaolinite, but an acid environment seems highly improbable unless achieved through some biogenic-related process.

Both pelletal and oolitic material are characterized by the presence of small amounts of calcite, cristobalite, illite, and some iron oxide. The calcite and cristobalite probably are replacement materials within the collophane. Illite probably was original material incorporated into the formation of pellets. In oolites, illite laths oriented concentrically within the oolite probably were accreted.

A very rough approximation of CO₂ content was determined following the peak-pair method of Gulbrandsen (1971). This method requires the measurement of the angular difference ($\Delta 2\theta$) between two X-ray diffraction peaks at $51.6^\circ 2\theta$ (410) and $53.1^\circ 2\theta$ (004). Results are plotted in figure 26. All plots show an average CO₂ content of about two to three percent. Such a small sampling and size of study area unfortunately prevents detection of lateral regional facies or environmental changes as shown by Gulbrandsen in the Idaho-Wyoming area.

Scanning Electron Microscopy

The scanning electron microscope was employed for the study of sub-microscopic features of the phosphoritic rocks. The Carmel Valley phosphoritic rocks viewed through the



$$\text{CO}_2 = 23.6341 - 14.7361(\Delta 2\theta)$$

Standard error of estimate of CO₂ = 0.5580

Figure 26. Determination of CO₂ content from $\Delta 2\theta(004)-(410)$ of carbonate-fluorapatite.

scanning electron microscope generally were devoid of crystalline form or clustering of apatite as shown within a broken phosphate pellet with grain inclusion(s) (fig. 27). Average EDAX analysis indicated an elemental make up of predominantly twice as much calcium with respect to phosphorus (fig. 28) with variable amounts of silica. Calcium with respect to phosphorus in carbonate-fluorapatite has an approximate ratio of two to one; the EDAX readout confirms this ratio. Figure 29 shows a possible clustering of material on probable diatom debris in a broken phosphate pellet (S60-14). The cluster area when analyzed indicated a high silica and aluminum content (fig. 30) so then probably is some clay mineral. It has been concluded that the Carmel Valley phosphoritic rocks photographed show no indication of authigenic crystalline apatite growth.

Origins of Phosphoritic Rocks and Conclusions

Several origins for the formation of bedded marine phosphates have been proposed. These include: 1) phosphate-rich coprolites, fecal pellets, and fecal mud which subsequently serve as centers for further diagenetic accumulation of phosphate (Moore, 1939; Dietz and others, 1942), 2) metasomatism involving the replacement of calcareous material by phosphate (Emigh, 1958; Ames, 1959; Pevear, 1966; D'Anglejan, 1968), 3) inorganic precipitation involving deep, phosphorus-rich, bottom waters upwelling and subsequently precipitating

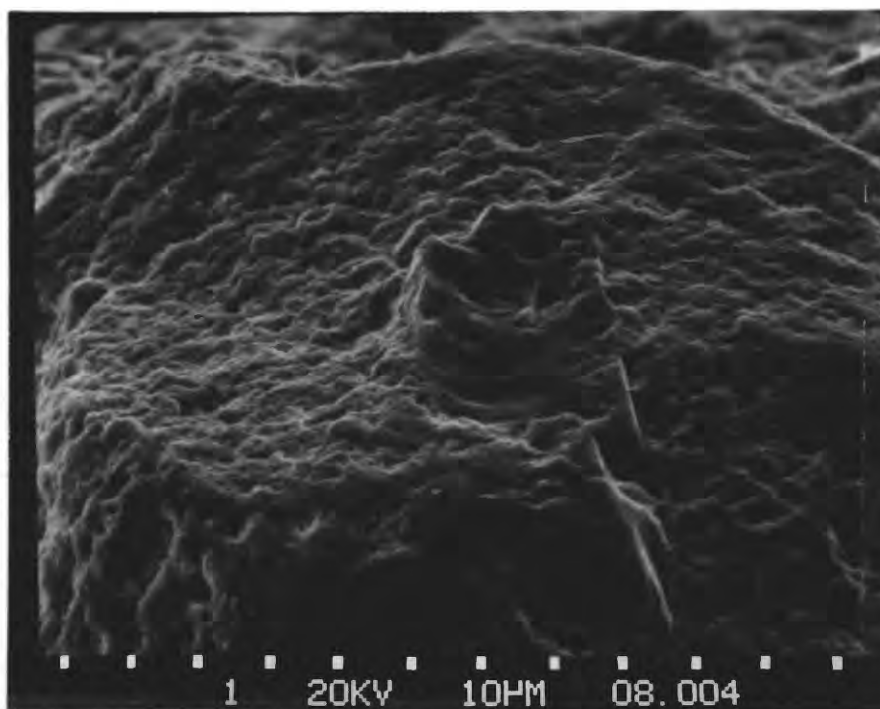


Figure 27. Pellet (S108) with grain inclusion showing massive character of collophane (10-micron spacing between tick marks).

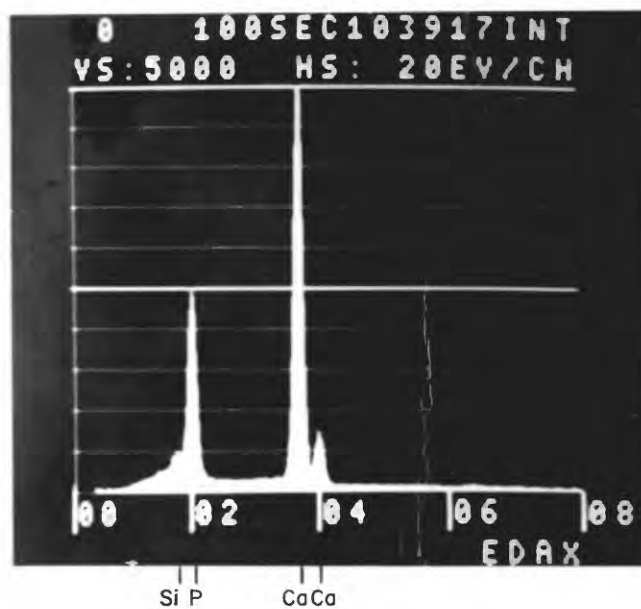


Figure 28. EDAX readout of pellet in figure 27 showing elemental composition of collophane.

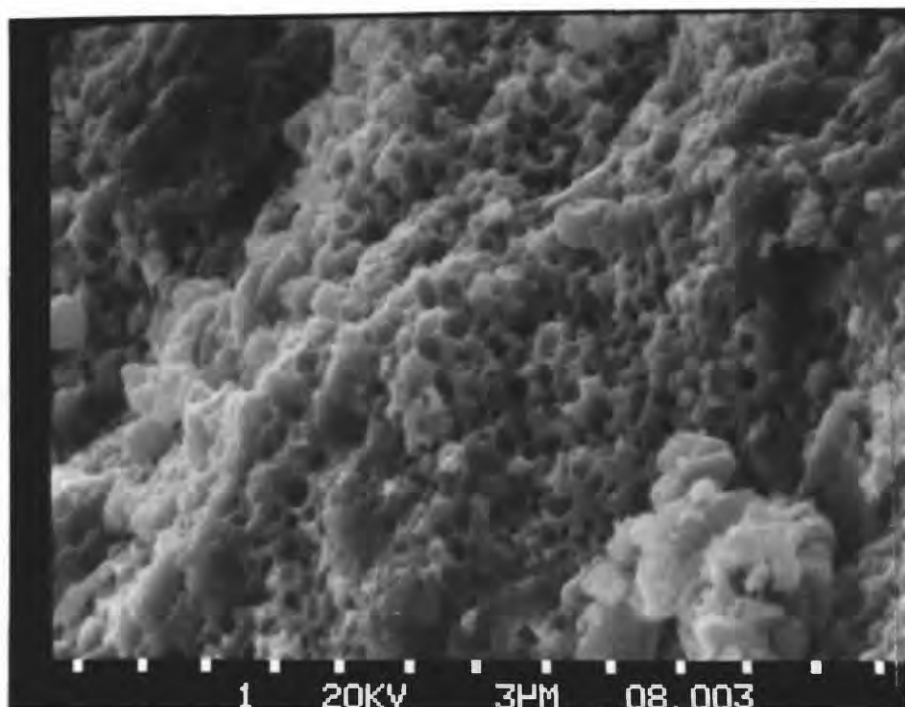


Figure 29. Pellet (S60-14) showing clustered material on probable diatom debris (3-micron spacing between tick marks).

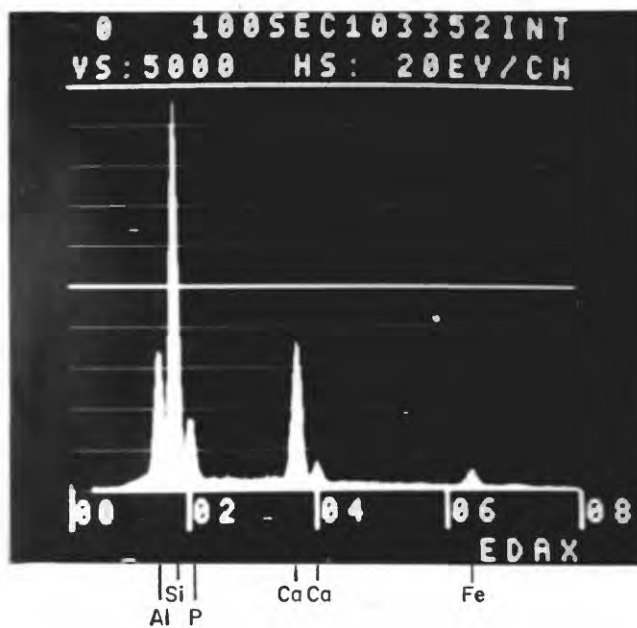


Figure 30. EDAX readout of clustered material in figure 29 showing elemental composition.

carbonate-fluorapatite (Kazakov, 1937; McKelvey and others, 1953; Gulbrandsen, 1969), and 4) a combination of inorganic precipitation and biogenic processes (McKelvey and others, 1959; Dickert, 1970; Cook, 1976; Burnett, 1974, 1977; Baturin and Bezrukov, 1979). Most emphasis on the origin of phosphates has been centered on a combination of inorganic precipitation and biogenic-related processes. Very briefly, a summation of conditions required for such a phosphate origin is: 1) a source of phosphorus supplied by phytoplankton related to upwelling and the subsequent death of these organisms, 2) anoxic conditions to retain concentrations of dead organisms which supersaturate interstitial and overlying waters with phosphorus, 3) alkaline conditions such that pH is greater than 7.2, 4) fairly warm water temperatures, 5) low partial pressures of CO₂, 6) formation in areas protected from terrigenous input, and 7) deposition in water depths ranging from 50 to 500 m. When such restrictive conditions are satisfied, precipitation of carbonate-fluorapatite may take place at the sediment water interface, but more probably within interstitial pore spaces in the sedimentary column. According to this hypothesis, such precipitation results in formation of phosphatic gels which construct soft bodies of various sizes which subsequently, through lithification and self-purification, harden and become enriched in P₂O₅ content. Initial phosphatic sediments are then further concentrated in amount of phosphatic material through reworking and winnowing caused by water flow actions.

This scheme of phosphate generation has been applied to the majority of known phosphate deposits, but does not appear to be the primary way in which the Carmel Valley phosphoritic rocks were formed. A direct biogenic origin for phosphate deposition has been mentioned, yet not seriously considered in recent literature. Lack of uncontested examples to substantiate such an origin have led many to consider the more accepted precipitation-organic related processes. The author is inclined to believe that the majority of phosphoritic rocks in the Robinson Canyon-Laureles Grade area are the result of direct organic processes, namely organic pelletization with subsequent metasomatic phosphate enrichment.

The author believes that the majority of phosphoritic rocks in the Carmel Valley area are the result of direct biogenic processes for several reasons. The majority of phosphoritic rocks in the Carmel Valley area are predominantly composed of pelletal phosphate. The striking feature of the Carmel Valley phosphoritic rocks is the size and shape of the pellets; generally ovoid, elongate, and ellipsoidal and from 0.1 mm to 1 mm, but more generally 0.3 to 0.7 mm in diameter. Very few are spherical in shape. This size and shape conforms with the morphology of excreted material by marine organisms. A large variety of marine organisms produce coherent fecal material which ranges in size from considerably less than 1 mm to 2 mm (Schrader, 1971; Pryor,

1975). Such organisms include bivalves, worms, gastropods (Hantzschel and others, 1968), echinoids, chitons, and certain arthropods (Hattin, 1975). The dominant type of fecal material produced by these organisms is an unsculptured pellet of the simple ovoid type (Moore, 1939).

The concentration of organic material, notably diatom debris within the Carmel Valley pellets is another characteristic feature (figs. 17 and 18). Diatoms are an important part of the marine food chain and in many cases are selectively fed upon by higher order organisms. A diet consisting of phytoplankton material and the subsequent excretion of concentrated diatom debris in the form of fecal pellets by zooplankton or other organisms is a natural, uncomplicated way of generating pelletal sediment enriched in organic debris. Undigested waste (Hattin, 1975), diatom concentrations, and in some instances complete diatom remains (Schrader, 1971), have been observed in modern fecal material.

Another internal feature common in many of the Carmel Valley pellets is a crude mosaic or grapestone structure (fig. 15). Such a feature may have been caused by mineral replacement processes, or possibly by organic digestive processes which involved wadding and packing of feces material into coherent fecal pellets (Pryor, 1975). Moore (1939) observed a definite sorting of coarser from finer material and the segregation of such material within fecal pellets. Modern deep sea fecal material shows internal almond or grapestone structure (Reineck and Singh, 1975).

The considerable scatter in P_2O_5 content (fig. 23) of the Carmel Valley phosphoritic rocks may be explained by biogenic pelletization. When phytoplankton are eaten by larger organisms, the phosphate contained in the phytoplankton is concentrated by a factor of up to 10^8 . Subsequently, this concentrated phosphate material is returned to the ocean as excreted material or liberated upon death and decomposition of the predator (Rhodes and Bloxam, 1969). The amount of concentrated phosphorus in excreted material differs with respect to the type of marine organism and its diet. Recent determinations of P_2O_5 content in fecal pellets range from 0.13 percent to 0.68 percent (Pryor, 1975), 0.21 to 0.42 percent (Takahashi and Yagi, 1929) to as high as 3.9 percent (Johannes and Satomi, 1966). In recent dog feces P_2O_5 content was as high as 31.5 percent (Williams, 1972). Fecal material can be a significant factor in the enrichment of sediments with organic material and phosphate as shown by Haven and Morales-Alamo (1968, 1970) in an estuary of the York River in Virginia.

The occurrences of many phosphoritic beds in close proximity to, if not adjacent to, thoroughly bioturbated clay mudstone zones within the Sandholdt Member suggests a strong relationship to organisms (plates 4 and 5). Zones of bioturbation in modern day oceans exhibit fluid, fecal pellet-rich surfaces that are easily resuspended by low velocity currents. In zones of extremely slow rates of sedimentation

where bioturbation is intensive, concentrated fecal pellets also occur (Reineck and Singh, 1975). The Carmel pelletal phosphate occurs in calcareous muds similar to that in deposits described by Dietz and others (1942) off the coast of California, which, presumably have a fecal origin.

The Carmel Valley pelletal phosphates have a large areal extent and foraminifers suggest a depth range from outer neritic to lower middle bathyal, or at depths of approximately 100 m to 2000 m. Many of the phosphoritic beds probably were emplaced by fluidized flows. Just how far phosphoritic material was transported remains unanswered. Modern day fecal pellets have been found at a wide range of depths, from tidal flats and lagoons, down to 4000 m on abyssal plains (Moore, 1939; Schrader, 1971; Reineck and Singh, 1975).

Concentrations of modern fecal pellets range from as few as 3.3 pellets per cm^3 to as many as 175 pellets per cm^3 (Moore, 1939). The concentration of pelletal material into distinct phosphoritic beds may not be due entirely to transport or current agencies, but may in part be due to initial deposition by organic processes. Verwey (1952) estimated that the Mytilus population in the Waddensee was capable of producing enough fecal material to cover an area of 600 km^2 to a depth of 0.25 mm in one year. Kornicker and Purdy (1957) reported thick sequences of sediment in the British West Indies region composed of 90 percent fecal pellets excreted by the marine gastropod Batillaria minima.

Frankenberg and others (1967) have reported Callianassa fecal pellet densities of 770,000 per m². Fecal muds as thick as 5 cm have been reported off the coast of Panama. These marine organisms show that fecal material can be generated in concentrations sufficient to form whole beds of fecal material which in turn could be transported to deeper waters by fluidized flow.

The stratigraphically restricted nature of the Carmel Valley phosphoritic beds may reflect intense organic processes during a cessation in terrigenous input. The only non-clay sediment developed may have been of an organic origin via fecal pelletization along with sparse grains which together supplied the bulk material for fluidized or grain flows. A subsequent rapid subsidence and change from calcareous to siliceous deposition in the study area probably altered the paleoecology to less hospitable or even toxic environments for the marine population and thus brought about an abrupt cessation in biogenic pelletization.

Important questions arise in a fecal pellet origin of the Carmel Valley pelletal phosphates. Just how resistant is fecal material when originally excreted and what are the possibilities of preservation or even transportation of such material intact? Modern day fecal pellets consist of an outer membrane (Schradler, 1971) or mucous-like organic slime which coats (Pryor, 1975) and protects the pellet from immediate attack by bacteria. Fecal pellets may further be

protected from predators which live on fecal material (Frankenberg and Smith, 1967) by sinking into or being transported into anoxic environments which may or may not be within the oxygen minimum zone. Moore (1939) noted that mud-eating polychaetes produced fairly resistant pellets, which in the past may have survived to become fossilized. He also reported that fecal pellets as old as 100 years may show no evidence of breakdown. Kornicker and Purdy (1957) noted the presence of hardened fecal pellets of Butillaria minima in sediment cores from the British West Indies region, and concluded that such fecal material was capable of preservation. It also is probable that fecal material may reside in a depositional environment long enough to be further metasomatically phosphatized and thus hardened prior to transport via fluidized flows. The fact that fecal material has been identified in Pleistocene (Pryor, 1975) and Cretaceous rocks (Hattin, 1975) as phosphatized fecal pellets (Cook, 1976) attests to their durability.

A transporting mechanism of fecal material other than sinking through the water column would be a fluidized sediment flow or grain flow. Concentrated fecal material probably would have a consistency very similar to loosely packed sand and thus might be subject to liquefaction. Fecal material entrained in such a transporting mechanism would be supported by pore fluid and thus behave like a fluid (Middleton and Hampton, 1973). Features present in the Carmel Valley

phosphoritic beds such as load casts, flame structures, suspended clasts, and water-escape structures are characteristic of grain flow or fluidized flows (Stauffer, 1967). The average thickness of phosphoritic beds of 5 to 7 cm conforms to Lowe's (1976) findings in which he emphasized a general thickness of 5 cm for grain flows. The other possibility of transport would be by turbidite mechanisms as indicated by graded bedding and abundance of matrix material in phosphoritic beds. The abundance of matrix material could have served as a cushion for fecal material during transport.

The most probable environment for oolites is in a tidal flat setting (Blatt and others, 1972), or possibly in a high to moderate energy shelf. Environments favorable for the concentration of fecal material are just seaward of a tidal flat. Oolitic material normally is rather rare in phosphorites (Cook, 1976), but in the overall Carmel Valley area such material accounts for 20 percent of the phosphate components. A mechanically accreted or snowball mechanism of phosphate addition has been pointed out (figs. 13 and 14).

In nearshore environments it is possible to have fecal muds not necessarily made up of pellets, but microspherite which is layered microcrystalline collophane (Freas, 1964). Many marine organisms such as gastropods produce fecal matter while still moving and thus generate threads of fecal matter (Moore, 1939; Reineck and Singh, 1975) which conceivably could develop into layers of microspherite material.

In a tidal environment, for instance, given sufficient microsporite material available for plastering, it seems possible that oolitic phosphate could be generated. Such accreted oolites may not be restricted to tidal flat environments, but could occur in deeper water environments. The zonation or ring-like structure emphasized by light and dark colored zones due to probable fluctuating oxidizing conditions, however, would tend to suggest a tidal flat environment rather than deeper water environments. The presence of kaolinite in oolites also may indicate close proximity to areas of terrigenous input or shoreline. Kaolinite may also result from organic processes related to digestive systems in organisms which have been shown to alter clay structures significantly (Pryor, 1975). The relative higher amounts of P_2O_5 content in oolites with respect to pellets may be the result of leaching of nonphosphatic components which would occur in tidal environments due to periodic subaerial exposure. The presence of oolitic material only on the north side of the Carmel Valley further suggests a shoaling in that direction.

Ghost and non-centered pelletal phosphate (figs. 16, 19-22) are probably secondary in situ phosphatic features. Irregularity of shape, poor sorting, fuzzy boundaries, similarity of composition of grain inclusions and exterior (of pellet) framework grains, and protruding and intruding detrital grains in non-centered pelletal phosphate are features

which indicate in situ phosphate deposition. The author speculates that such in situ phosphate generation probably developed from interstitial pore waters saturated with phosphorus derived from the original, phosphatic, fecal pelletal material. Phosphatic intraclasts in the form of gravels and pebbles represent lithified fecal pelletal material and possibly liberated pseudo-nodules which were ripped up and re-deposited by bottom currents or possibly turbidity currents.

In conclusion, the majority of the Robinson Canyon-Laureles Grade area phosphoritic rocks probably have a fecal pellet origin. Pre-concentrated fecal pelletal sediment supplemented also by shallow water-generated oolites supplied the bulk of the material which was subsequently transported from shallower waters (less than 300 m) to a wide range of deeper bathyal environments. The paleogeographic setting during deposition of the phosphoritic beds probably was that of a continental borderland, the Carmel Valley probably representing a restricted or silled basin characterized by steep slopes suitable for the generation of fluidized flows or grain flows. Incorporated within these flows also were minor amounts of much more lithified, phosphatic intraclasts. Once final deposition had taken place within this basin, minor amounts of secondary phosphate pellets formed, supplemented with possible further enrichment of the original fecal pellets in P_2O_5 through metasomatic processes. Figures 31 and 32 summarize the author's interpretations of the origin and transport of the Carmel Valley phosphoritic rocks.

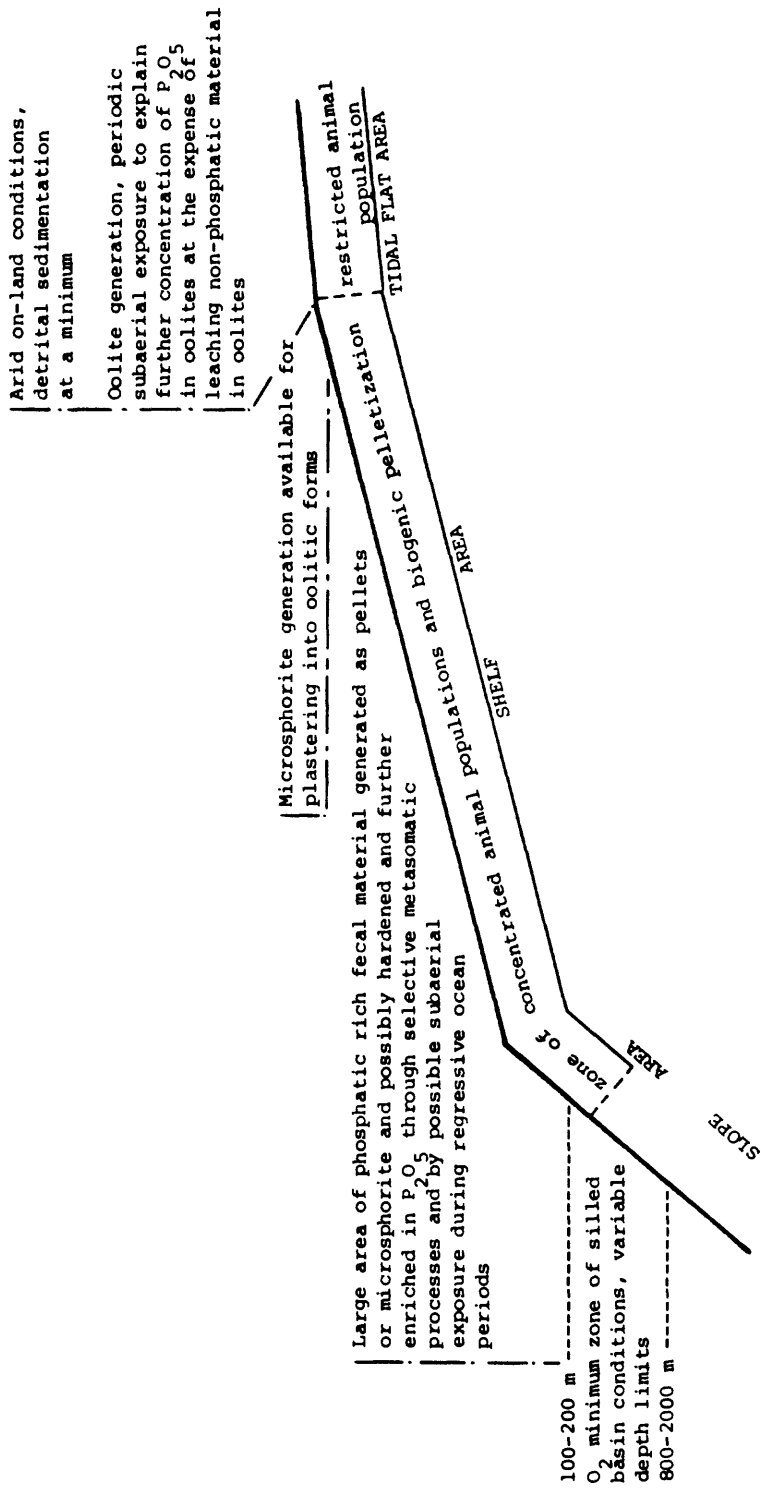


Figure 31. Model of phosphoritic rock genesis in the Robinson Canyon-Laureles Grade area (inclination of shelf and slope areas greatly exaggerated).

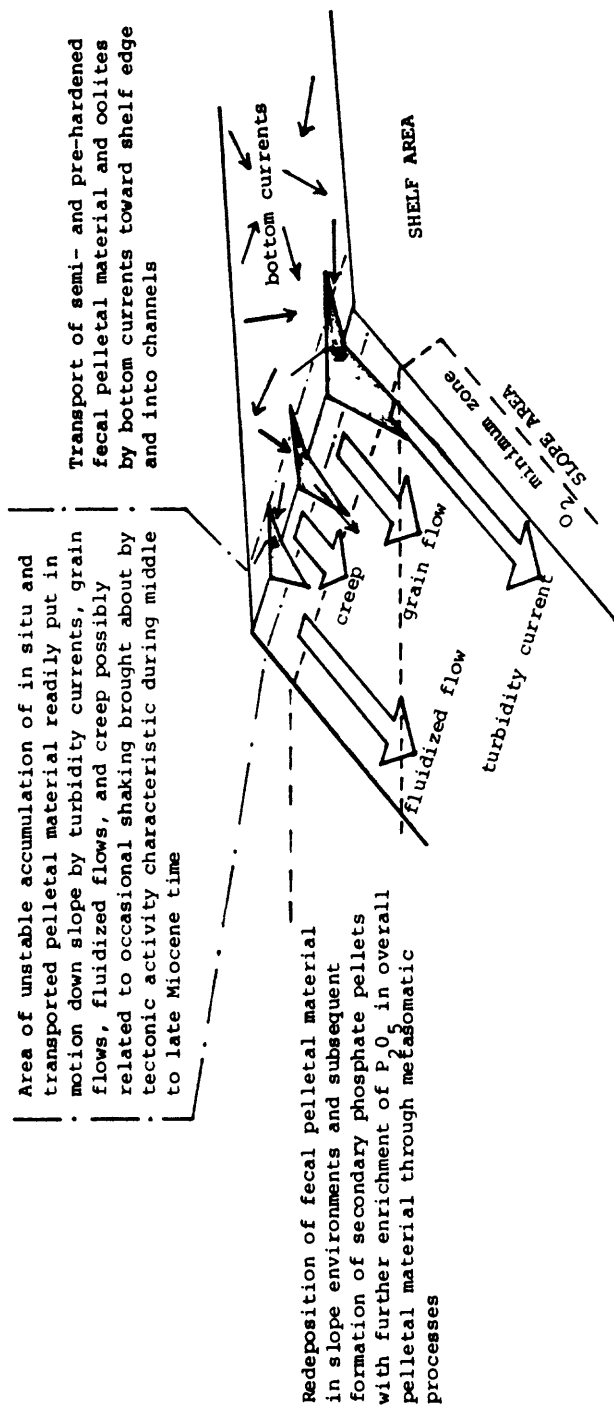


Figure 32. Model of transport and final deposition of the phosphoritic rocks in the Robinson Canyon-Laureles Grade area.

REFERENCES CITED

- Altschuler, Z.S., Clarke, R.S., Jr., and Young, E.J., 1958, Geochemistry of uranium in apatite and phosphorite: U.S. Geological Survey Professional Paper 314-D, p. D45-D90.
- Ames, L.L., 1976, The genesis of carbonate apatites: *Economic Geology*, v. 54, no. 5, p. 829-841.
- Arnal, R.E., 1976, Miocene paleobathmetric changes of the Santa Rosa-Cortes Ridge area, California continental borderland: *American Association of Petroleum Geologists, Miscellaneous Publication 24*, p. 60-79.
- Baturin, G.N., and Bezrukov, P.L., 1979, Phosphorites on the sea floor and their origin: *Marine Geology*, v. 31, p. 317-332.
- Blake, W.P., 1856, Notice of remarkable strata containing the remains of Infusoria and Polythalamia in the Tertiary formation of Monterey, California: *Academy of Natural Science Philadelphia Proceedings*, v. 7, p. 328-331.
- Blatt, H., Middleton, G., and Murray, R., 1972, *Origin of sedimentary rocks: Englewood Cliffs, New Jersey, Prentice Hall*, 634 p.
- Bouma, A.H., 1962, *Sedimentology of some flysch deposits: Amsterdam, Elsevier*, 168 p.
- Bowen, O.E., 1965, Stratigraphy, structure and oil possibilities in the Monterey and Salinas quadrangles, California: A symposium of papers presented at the 40th annual Pacific Section American Association of Petroleum Geologists convention, 1965, p. 48-67.
- Bramlette, M.N., 1946, The Monterey Formation of California and the origin of its siliceous rocks: U.S. Geological Survey Professional Paper 212, 57 p.
- Brown, E.H., 1962, The geology of the Rancho San Carlos area, Monterey County, California: Unpublished student report, Stanford University, 56 p.
- Burnett, W.C., 1974, Phosphorite deposits from the sea floor off Peru and Chile; radiochemical and geochemical investigations concerning their origin: Hawaii Institute of Geophysics, University of Hawaii, HIG-74-3, 164 p.

- Burnett, W.C., 1977, Geochemistry and origin of phosphorite deposits from off Peru and Chile: Geological Society of America Bulletin, v. 88, no. 6, p. 813-823.
- Carozzi, A.V., 1960, Microscopic sedimentary petrography: New York and London, John Wiley and Sons Inc., 485 p.
- Cassell, J.K., 1949, Variation of the type Monterey Formation, California, near the type locality [M.Sc. thesis]: Stanford, Calif., Stanford University, 44 p.
- Cathcart, J.B., and Gulbrandsen, R.A., 1973, Phosphate deposits: U.S. Geological Survey Professional Paper 820, p. 515-525.
- Clark, J.C., Dibblee, T.W., Jr., Greene, H.G., and Bowen, O.E., Jr., 1974, Preliminary geologic map of the Monterey and Seaside 7.5 minute quadrangles, Monterey County, California, with emphasis on active faults: U.S. Geological Survey Miscellaneous Field Studies Map MF-577, 2 sheets.
- Compton, R.R., 1966, Granitic and metamorphic rocks of the Salinian Block, California Coast Ranges: California Division of Mines and Geology Bulletin, no. 190, p. 277-287.
- Cook, P.J., 1976, Sedimentary phosphate deposits, Handbook of strata-bound and stratiform ore deposits; II. Regional studies and specific deposits; v. 7, Au, U, Fe, Mn, Hg, Sb, W, and P deposits (Wolf, K.H., editor): New York, Elsevier, p. 505-535.
- D'Anglejan, B.F., 1968, Phosphate diagenesis of carbonate sediments as a mode of in situ formation of marine phosphorites-observations from the eastern Pacific: Canadian Journal of Earth Sciences, v. 5, no. 1, p. 81-87.
- Dickert, P.F., 1970, Neogene phosphate facies in California [Ph.D. thesis]: Stanford, Calif., Stanford University, 305 p.
- Dietz, R.S., Emery, K.O., and Shepard, F.P., 1942, Phosphorite deposits on the sea floor of southern California: Geological Society of America Bulletin, v. 53, p. 815-848.
- Durham, D.L., 1974, Geology of the southern Salinas Valley area, California: U.S. Geological Survey Professional Paper 819, 111 p.

- Emigh, G.D., 1958, Petrography, mineralogy and origin of phosphate pellets in the Phosphoria Formation: Idaho Bureau of Mines and Geology Pamphlet 114, 60 p.
- Fiedler, W.M., 1944, Geology of the Jamesburg quadrangle, Monterey County, California: California Journal of Mines and Geology, v. 40, no. 2, p. 177-250.
- Folk, R.L., 1974, Petrology of sedimentary rocks: Austin, Texas, Hemphill Publishing Co., 182 p.
- Frankenberg, D., and Smith, K.L., Jr., 1967, Coproghagy in marine animals: Limnology and Oceanography, v. 12, p. 443-450.
- Frankenberg, D., Coles, S.L., and Johannes, R.E., 1967, The potential trophic significance of Callianassa major fecal pellets: Limnology and Oceanography, v. 12, p. 113-120.
- Freas, D.H., 1964, Stratigraphy and sedimentation of phosphorite in the central Florida phosphate district (abs.): Economic Geology, v. 59, p. 1619.
- Galliher, E.W., 1930, A study of the Monterey Formation, California, at the type locality [M.Sc. thesis]: Stanford, Calif., Stanford University, 29 p.
- _____, 1931, Collophane from Miocene brown shales of California: American Association of Petroleum Geologists Bulltetin, v. 15, no. 3, p. 257-269.
- _____, 1932, Geology and physical properties of building stone from Carmel Valley, California: Report 28 of the State Mineralogists, California Journal of Mines and Geology, v. 28, no. 1, 25 p.
- Geological Society of America, 1963, Rock color chart: Geological Society of America, Boulder, Colorado.
- Gower, H.D., and Madsen, B.M., 1964, The occurrence of phosphate in California; in short papers in geology and hydrology: U.S. Geological Survey Professional Paper 501D, p. D79-D85.
- Graham, S.A., 1976, Tertiary sedimentary tectonics of the central Salinian Block of California [Ph.D. thesis]: Stanford, Calif., Stanford University, 465 p.

- Graham, S.A., 1978, Role of Salinian Block in evolution of the San Andreas Fault system, California: American Association of Petroleum Geologists Bulletin, v. 62, no. 11, pt. 1, p. 2241-2231.
- Gulbrandsen, R.A., 1969, Physical and chemical factors in the formation of marine apatite: Economic Geology, v. 64, no 4, p. 365-382.
- _____, 1971, Relation of carbon dioxide content of apatite of the Phosphoria Formation to regional facies: Mountain Geologist, v. 8, no. 2, p. 81-84.
- Hanna, G.D., 1928, The Monterey Shale of California at its type locality with a summary of its fauna and flora: American Association of Petroleum Geologists Bulletin, v. 12, no. 10, p. 969-983.
- Hantzschel, W., Farouk, E., and Amstutz, G.C., 1968, Coprolite: An annotated bibliography: Geological Society of America Memoir 108, 132 p.
- Hattin, D.E., 1975, Petrology and origin of fecal pellets in upper Cretaceous strata of Kansas and Saskatchewan: Journal of Sedimentary Petrology, v. 45, no. 3, p. 686-696.
- Haven, D.E., and Morales-Alamo, R., 1968, Occurrence and transport of faecal pellets in suspension in a tidal estuary: Sedimentary Geology, v. 2, p. 141-151.
- _____, 1970, Filtration of particles from suspension by the American oyster Crassostrea virginica: Biological Bulletin, v. 139, p. 248-264.
- Johannes, R.E., and Satomi, M., 1966, Composition and nutritive value of fecal pellets of a marine crustacean: Limnology and Oceanography, v. 11, p. 191-197.
- Kazakov, A.V., 1937, The phosphorite facies and the genesis of phosphorites, in Geological investigations of agricultural ores USSR: Science Institute of Fertilizers and Insectofungicides Translations (USSR), no. 142, p. 95-113.
- Kleinpell, R.M., 1938, Miocene stratigraphy of California: Tulsa, Oklahoma, American Association of Petroleum Geologists, 450 p.
- Kornicker, L.S., and Purdy, E.G., 1957, A Bahamian faecal-pellet sediment: Journal of Sedimentary Petrology, v. 27, no. 2, p. 126-129.

- Lawson, A.C., 1893, The geology of Carmelo Bay: California University Department of Geological Sciences Bulletin, v. 1, p. 1-59.
- Louderback, G.D., 1913, The Monterey Series in California: California University Department of Geology Bulletin, v. 7, no. 10, p. 177-241.
- Lowe, D.R., 1976, Grain flow and grain flow deposits: Journal of Sedimentary Petrology, v. 46, no. 1, p. 188-199.
- McKelvey, V.E., Swanson, R.W., and Sheldon, R.P., 1953, The Permian phosphate deposits of Western United States: International Geological Congress, 19th Comptes rendus, section 11, pt. 11, p. 45-64.
- McKelvey, V.E., and others, 1959, The Phosphoria Park City and Shedhorn Formations, in the Western Phosphate Field: U.S. Geological Survey Professional Paper 313A, 47 p.
- Maher, J.C., 1959, The composite interpretive method of logging of drill cuttings: Oklahoma Geological Survey Guidebook 8, 48 p.
- Martin, B., 1912, Fauna from the type locality of the Monterey Series in California: University of California Publications in Department of Geology, v. 7, no. 7, p. 143-150.
- Mason, B., 1966, Principles of geochemistry: New York, John Wiley and Sons Inc., 3rd edition, 329 p.
- Middleton, G.V., and Hampton, M.A., 1973, Mechanics of flow and deposition: Society of Economic Paleontologists and Mineralogists, Pacific Section, short course, Anaheim 1973, Turbidites and Deep Water Sedimentation, p. 1-38.
- Moore, H.B., 1939, Faecal pellets in relation to marine deposits; in Recent marine sediments, a symposium (editor Parker D. Trask): American Association of Petroleum Geologists, p. 516-523.
- Murata, K.J., and Larson, R.R., 1975, Diagenesis of Miocene siliceous shales, Temblor Range, California: U.S. Geological Survey Journal of Research, v. 3, no. 5, p. 553-566.
- Murata, K.J., and Norman, M.B., II, 1976, An index of crystallinity for quartz: American Journal of Science, v. 276, no. 9, p. 1120-1130.

- Murata, K.J., and Randall, R.G., 1975, Silica mineralogy and structure of the Monterey Shale, Temblor Range, California: U.S. Geological Survey Journal of Research, v. 3, no. 5, p. 567-572.
- Neel, T.H., 1963, Geology of the lower Tularcitos Creek-Cachagua Grade area, Jamesburg quadrangle, California [M.Sc. thesis]: Stanford, Calif., Stanford University, 45 p.
- Pevear, D.R., 1966, The estuarine formation of U.S. Atlantic coastal plain phosphorite: Economic Geology, v. 61, p. 251-256.
- Powers, M., 1953, A new roundness scale for sedimentary particles: Journal of Sedimentary Petrology, v. 23, p. 117-119.
- Pryor, W.A., 1975, Biogenic sedimentation and alteration of argillaceous sediments in shallow marine environments: Geological Society of America Bulletin, v. 86, p. 1244-1254.
- Reineck, H.E., and Singh, I.B., 1975, Depositional sedimentary environments: New York, Springer-Verlag, 439 p.
- Rhodes, R.H.T., and Bloxam, T., 1969, Phosphatic organisms in the Paleozoic and their evolutionary significance: Symposium North American Paleontological Convention, Part K, p. 1485-1513.
- Rogers, A.F., 1944, Pellet phosphorite from Carmel Valley, Monterey County, California: California Journal of Mines and Geology, v. 40, no. 4, p. 411-421.
- Rooney, T.P., and Kerr, P.F., 1967, Mineralogic nature and origin of phosphorite, Beaufort County, North Carolina: Geological Society of America Bulletin, v. 78, p. 731-748.
- Ross, D.C., 1973, Are the granitic rocks of the Salinian Block trondjemitic: U.S. Geological Survey Journal of Research, v. 1, no. 3, p. 251-254.
- _____, 1976a, Reconnaissance geologic map of pre-Cenozoic basement rocks, northern Santa Lucia Range, Monterey County, California: U.S. Geological Survey Miscellaneous Field Studies Map MF 750.

- Ross, D.C., 1976b, Metagraywacke in the Salinian Block, central Coast Ranges, California and a possible correlative across the San Andreas Fault: U.S. Geological Survey Journal of Research, v. 4, no. 6, p. 638-696.
- Ross, D.C., and Brabb, E.E., 1973, Petrography and structural relations of granitic basement rocks in the Monterey Bay area, California: U.S. Geological Survey Journal of Research, v. 1, no. 3, p. 273-282.
- Sandberg, C.A., and Gutschick, R.C., 1977, Paleotectonic, biostratigraphic, and economic significance of Osagean to early Meramecian starved basin in Utah: U.S. Geological Survey Open-file Report 77-121, 16 p.
- Schrader, H.J., 1971, Fecal pellets: Role in sedimentation of pelagic diatoms: Science, v. 174, p. 55-57.
- Seilacher, A., 1967, Bathymetry of trace fossils: Marine Geology, v. 5, p. 413-428.
- Service, A.L., and Popoff, C.C., 1964, An evaluation of the western phosphate industry and its resources (in five parts). 1. Introductory review: U.S. Bureau of Mines Report of Investigations 6485, 86 p.
- Sieck, H.C., 1964, A gravity investigation of the Monterey-Salinas area: Unpublished student report, Stanford University, 39 p.
- Stauffer, P.H., 1967, Grain flow deposits and their implications: Journal of Sedimentary Petrology, v. 37, p. 487-508.
- Takahashi, J., and Yagi, T., 1929, Peculiar mud grains and their relation to the origin of glauconite: Economic Geology, v. 24, no. 8, p. 338-352.
- Thorup, R.R., 1976, Groundwater study of the Carmel Valley Ranch and Carmel River watershed, Monterey Peninsula, Monterey County, California: Unpublished private report done for Mr. D. Kaye Chandler of the Unique Golf Concepts, Inc., 2252 Fremont Street, Monterey, California 93940.
- Trask, P.D., 1925, Geology of the Point Sur quadrangle, California: University of California Department of Geology Bulletin, v. 16, p. 119-186.

- Vail, P.R., Mitchum, R.M., Jr., and Thompson, S., III, 1977, Seismic stratigraphy and global changes of sea level, part 4, in Global cycles of relative changes of sea level: American Association of Petroleum Geologists Memoir 26, p. 83-96.
- Verwey, J., 1952, On the ecology of distribution of cockle and mussel in the Dutch Waddensee, their role in sedimentation and source of their food supply: Leiden, Archiv. Neerland. Zoology, v. 10, p. 171-240.
- Walker, T.R., 1967, Formation of red beds in modern and ancient deserts: Geological Society of America Bulletin, v. 78, p. 353-368.
- Wentworth, C.K., 1922, A scale of grade and class terms for clastic sediments: Journal of Geology, v. 30, p. 377-392.
- Wiebe, R.A., 1970, Pre-Cenozoic tectonic history of the Salinian block, western California: Geological Society of America Bulletin, v. 81, no. 6, p. 1837-1842.
- Wiedmann, J.P., 1964, Geology of the upper Tularcitos Creek-Cachagua Creek area, Jamesburg quadrangle, California [M.Sc. thesis]: Stanford, Calif., Stanford University, 62 p.
- Williams, H., Turner, F., and Gilbert, C., 1954, Petrography, an introduction to the study of rocks in thin section: San Francisco, W.H., Freeman and Company, 406 p.
- Williams, J.W., 1970, Geomorphic history of Carmel Valley and Monterey Peninsula, California [Ph.D. thesis]: Stanford, Calif., Stanford University, 106 p.
- Williams, M.E., 1972, The origin of spiral coprolites: University of Kansas Paleontological Contributions, no 59, 19 p.

APPENDIX 1

Laboratory Work and Procedures

Representative rock samples were slabbed for etching and staining in order to emphasize internal structures and to aid in preparing descriptions of phosphoritic rocks. Granitic slabs were etched in HF and stained with cobaltinitrite solution in order to determine K-spar content. Plagioclase content in granitic rocks was determined by etching rocks with BaCl and subsequently staining with Aramath dye. Rocks were slabbed both at San Jose State University and at the U.S. Geological Survey in Menlo Park.

Thin sections were made at San Jose State University and petrographic work was done at the U.S. Geological Survey in Menlo Park. Sedimentary rock names proposed by Folk (1974) were used to describe rocks studied in thin section. Estimations of sorting, component percent distributions, pore space, and compaction are based on a count of three hundred points in thin sections at a set interval of 0.5 mm. Photomicrographs were taken of representative slides.

Semiquantitative chemical analyses on selected phosphoritic rock samples were performed at the U.S. Geological Survey facilities in Menlo Park, California, and Reston, Virginia. Nine elements, Si, Al, Na, K, Fe, Mg, Ca, Ti, and P, with relative percentages were reported, and these percentages then were converted into common oxides.

Samples selected for X-ray diffraction were analyzed at Menlo Park. Both whole rock analyses and isolated oolite-pellet phosphate analyses were performed. Oolite and pellet phosphates were segregated from whole rock samples by disaggregation and subsequent screening; further concentration of pellets and oolites was accomplished by floating off equivalent sized quartz and feldspars in bromoform. Samples were crushed and mounted in aluminum planchets. A Norelco X-ray diffraction spectrometer using nickel-filtered copper K α radiation was used; scan rates were one degree 2 θ per minute and one half degree 2 θ per minute. Diatomite, porcelanite, and chert samples also were analyzed by X-ray diffraction methods; scan rates were one fourth degree 2 θ per minute.

Phosphoritic samples analyzed under the scanning electron microscope were mounted on aluminum plates and carbon coated. The elemental makeup of the phosphate constituents was obtained through analysis by a supplementary energy dispersive X-ray unit (EDAX) attached to the scanning electron microscope. Photographs were taken both from the scanning electron microscope and of EDAX readouts of selected samples.

Invertebrate megafossil samples collected were identified by matching with photographs and descriptions of forms included in previous faunal lists of the study area. Samples collected for microfossil content were disaggregated, washed, and screened at the author's residence. Disaggregation was accomplished by soaking air dried samples in kerosene; subsequently the kerosene was replaced by warm water, and then the samples were heated to near boiling for approximately two hours on an oscillating hot plate. Samples then were cooled, washed, and wet sieved between a 32 mesh (0.495 mm) and 200 mesh (0.074 mm) gauge sieves and left to air dry. Once dry, samples were screened, picked, and identified.

APPENDIX 2

Test Well Data (Thorup, 1976)

LOCATION: 1500 ft E and 2350 ft S of NW corner of Sec
25/T16S/1E on the east bank of Robinson Canyon
3500 ft south of Farm Center.

SURFACE ELEVATION: 250 ft

APPROXIMATE STANDING WATER LEVEL: 140 ft

TOTAL DEPTH: 600 ft

ELECTRIC LOG RUN: to a depth of 594 ft on September 24, 1974.

LITHOLOGY: (based on samples and electric log)

0-130	Sandstone, bluish gray and light gray, soft to hard. Water at 140 ft.
130-190	Sandstone, hard with shale streaks.
190-290	Sandstone with granitic debris.
290-305	Claystone
305-325	Sandstone, medium-grained, grains rounded.
325-420	Sandstone, coarse, gray, appears nonmarine and permeable.
420-450	Interbedded red clay, minor sandstone.
450-530	Interbedded red clay and coarse sandstone, hard.
530-600	Sand and gravel, red claystone on bottom.

GEOLOGIC STRUCTURE: Synclinal

ESTIMATED DEPTH TO GRANITE: 700 ft

DATE OF DRILLING: September 18, 1974 to September 24, 1974

APPENDIX 3

Paleobathymetry Determined From Foraminifers (based on
Arnal, 1976)

Sample Locality	Age	Paleodepth (m)
Mf-Y-462	middle Luisian	upper bathyal 200-600
Mf-Y-520	middle Luisian	outer neritic 100-200
Mf-Y-109-3	middle Luisian	upper bathyal 200-600
Mf-D-57	middle Luisian	upper bathyal 200-600
Mf-Y-191-1	upper Luisian	outer neritic 100-200
Mf-Y-191-8	upper Luisian	outer neritic 100-200
Mf-Y-60-2	upper Luisian	outer neritic 100-200
Mf-Y-60-6	upper Luisian	outer neritic 100-200
Mf-Y-60-9	upper Luisian	outer neritic 100-200
Mf-Bo-41	lower Mohnian	upper middle bathyal 500-1500
Mf-Bo-36	lower Mohnian	upper middle bathyal 500-1500
Mf-C-564	lower Mohnian	upper middle bathyal 500-1500
Mf-C-565	lower Mohnian	upper bathyal 200-600
Mf-C-566	lower Mohnian	upper bathyal 200-600
Mf-Y-228-2	lower Mohnian	outer neritic 100-200
Mf-Y-191-10	lower Mohnian	outer neritic 100-200
Mf-Y-60-10	lower Mohnian	outer neritic 100-200
Mf-Y-60-17	lower Mohnian	outer neritic 100-200
Mf-K-14	upper Mohnian	lower middle bathyal 1500-2000
Mf-Y-332-4	upper Mohnian	non-diagnostic depth indicators
Mf-Y-332-6	upper Mohnian	non-diagnostic depth indicators
Mf-C-567	upper Mohnian	upper middle bathyal 500-1500

APPENDIX 4

<u>Measured Section 8</u>	Thickness (m)
(Hames Member continues upward)	
45. Porcelanite, very light gray (N8), in 5- to 6-cm-thick beds.....	3.5
44. Pelletal phosphoritic sandstone.....	7.5 cm
43. Porcelanite, same as unit 45.....	0.6
42. Pelletal phosphoritic sandstone, same as unit 44.....	7.5 cm
41. Porcelanite, same as unit 45.....	1
Hames Member (beds 41-45)	
40. Claystone, siltstone, yellowish-gray (5Y7/2), in 5-to 6-cm-thick beds, in part laminated, siliceous, sparse pelecypods.....	5.7
39. Claystone, shale, yellowish gray (5Y7/2), in part laminated, siliceous....	0.6
38. Limestone bleb zone.....	0.3
37. Claystone, shale, same as unit 39.....	1
36. Siltstone, yellowish gray (5Y7/2), laminated, friable, calcareous.....	2
35. Sandstone, pale yellowish orange (10YR8/6), fine grained, good sorting, subangular to subrounded, siliceous.....	7.5 cm
34. Claystone, shale, same as unit 39.....	2
33. Siltstone, same as unit 36.....	1.7
32. Sandstone, same as unit 35, weakly calcareous.....	5 cm
31. Siltstone, same as unit 36.....	1.2
30. Sandstone, same as unit 32.....	0.3
29. Siltstone, same as unit 36.....	0.3
28. Limestone bleb zone.....	10 cm
27. Siltstone, same as unit 36.....	0.7
26. Sandstone, same as unit 35, calcareous...	5 cm
25. Siltstone, same as unit 36.....	1.2
24. Sandstone, same as unit 26.....	0.3
23. Siltstone, same as unit 36.....	1.4
22. Sandstone, same as unit 26.....	10 cm
21. Siltstone, same as unit 36.....	0.4
20. Sandstone, pale yellowish orange (10YR8/6), medium to fine grained, good sorting, graded, laminated in upper part, predominantly subangular to subrounded quartz, calcareous.....	0.6
19. Sandstone sequence same as in unit 20....	0.8

Measured Section 8 cont'd	Thickness (m)
18. Siltstone, same as unit 36.....	1
17. Sandstone, same as unit 26.....	7.5 cm
16. Siltstone, same as unit 36, phosphatic.....	1
15. Sandstone, same as unit 26.....	12.5 cm
14. Porcelanite, same as unit 45.....	1
13. Siltstone, same as unit 16.....	1.2
12. Sandstone, moderate pink (5YR7/4), medium grained, fair sorting, arkosic, weakly calcareous, crossbedded, grains subangular.....	12.5 cm
11. Siltstone, same as unit 16.....	2.1
10. Gypsum.....	2.5 cm
9. Limestone bleb zone.....	0.2
8. Siltstone, same as unit 16.....	0.2
7. Sandstone, same as unit 26.....	0.2
6. Siltstone, same as unit 16.....	1.2
5. Sandstone, same as unit 26.....	12.5 cm
4. Siltstone, same as unit 16.....	0.4
3. Sandstone, same as unit 20.....	0.4
2. Sandstone, pale yellowish orange (10YR8/6), medium to fine grained, good sorting, massive, friable, pre- dominantly subangular quartz, feldspar, little biotite, calcareous, phosphatic, carbonaceous, fish scales.....	1
1. Sandstone, same as unit 2, contains several gypsum interbeds 2.5 cm thick....	1

Sandholdt Member (beds 1-40)

(Dirt road base, Sandholdt Member possibly con-
tinues downward)

Total thickness..... 37.5

Measured Section 60

Thickness (m)

(Hames Member continues upward)

40. Claystone and porcelanite, very light gray (N8), in 5-to 6-cm-thick beds, few or no shale partings..... 4

Hames Member (bed 40)

39. Limestone bleb zone..... 10 cm
 38. Claystone and porcelanite, same as unit 40..... 1
 37. Siltstone, very pale orange (10YR8/2), and fine sandstone, shaly in part, friable, calcareous, phosphatic, contains foraminifers..... 1
 36. Limestone bleb zone..... 12.5 cm
 35. Siltstone, same as unit 37..... 1.5
 34. Covered..... 9.1
 33. Claystone, very pale orange (10YR8/2), in 8-to 16-cm-thick beds, siliceous, contains fish scales..... 0.6
 32. Claystone and porcelanite, same as unit 40, contains 0.5-to 1-cm-thick shale interbeds, laminated in part..... 0.5
 31. Claystone, same as unit 33..... 0.3
 30. Pelletal phosphoritic sandstone..... 10 cm
 29. Claystone and shale, very pale orange (10YR8/2), friable, weakly calcareous..... 1.8
 28. Shale and fine sandstone, very pale orange (10YR8/2), friable, calcareous.... 1.2
 27. Sandstone, very pale orange (10YR8/2), fine grained, good sorting, massive, friable, calcareous, grains subangular to subrounded..... 1.8
 26. Bedding plane fault zone..... 0.5
 25. Claystone, same as unit 33..... 0.6
 24. Claystone and shale, very pale orange (10YR8/2), in 18-to 20-cm-thick beds, siliceous, contains gastropods and pelecypods..... 1.2
 23. Pelletal phosphoritic sandstone, same as unit 30..... 7.5 cm
 22. Claystone and porcelanite, same as unit 32..... 0.6
 21. Claystone and shale, same as unit 29, contains shale interbeds which decrease in frequency up section, calcareous, phosphatic, carbonaceous, contains foraminifers..... 7.9

Measured Section 60 cont'd		Thickness (m)
20.	Whale bone horizon.....	0.2
19.	Claystone, shale, and fine sandstone, grayish orange (5YR8/2), less sand up section, rhythmic bedding, 1-to 5-cm-thick beds of alternating sandstone-shale sequences, calcareous, phosphatic, contains foraminifers.....	4
18.	Sandstone, very pale orange (10YR8/2), fine grained, good sorting, friable, predominantly subangular quartz, feldspar, and some biotite.....	0.2
17.	Claystone and shale, same as unit 29, calcareous, contains fish scales.....	0.5
16.	Limestone bleb zone.....	0.2
15.	Claystone and shale, same as unit 17.....	0.6
14.	Sandstone, same as unit 18.....	0.2
13.	Claystone and shale, same as unit 17.....	0.5
12.	Sandstone and siltstone, very pale orange (10YR8/2), very fine grained, good sorting, friable, laminated, predominantly subangular quartz, feldspar, some biotite, calcareous, phosphatic.....	1.5
11.	Sandstone, same as unit 18.....	0.3
10.	Sandstone and siltstone, same as unit 12, non-calcareous.....	1.8
9.	Sandstone, same as unit 18.....	1.7
8.	Sandstone and siltstone, same as unit 10.....	1
7.	Claystone, very pale orange (10YR8/2), partly laminated, weakly calcareous, contains small pelecypods, less common occurrence of thin 5-to 6-cm-thick fine sandstone interbeds.....	1.8
6.	Claystone, same as unit 7, lacks sandstone interbeds, contains less common occurrences of 5-to 6-cm-thick porcelanite interbeds, calcareous, contains foraminifers.....	2.1
5.	Sandstone, same as unit 18, calcareous.....	7.5 cm
4.	Claystone, same as unit 7, lacks sandstone interbeds.....	1.2
3.	Covered.....	30
2.	Claystone, same as unit 4.....	0.5

Measured Section 60 cont'd

Thickness (m)

Sandholdt Member (beds 2-39)

1. Sandstone, very pale orange (10YR8/2), coarse grained, fair sorting, predominantly subangular to subrounded quartz, feldspar, some biotite, phosphatic, contains pectens..... 4.5

Los Tularcitos Member (bed 1)

(Bottom of creek bed, Los Tularcitos Member possibly continues downward)

Total thickness..... 87

Measured Section 109

Thickness (m)

(Hames Member continues upward)

25. Porcelanite, very light gray (N8),
in 3-to 5-cm-thick beds..... 3

Hames Member (bed 25)

24. Covered..... 31
 23. Claystone, very light gray (N8),
massive, friable, calcareous..... 0.6
 22. Limestone..... 0.2
 21. Claystone, same as unit 23..... 3.6
 20. Porcelanite, same as unit 25..... 0.2
 19. Claystone, same as unit 23, but
silty and in part shaly..... 0.8
 18. Limestone..... 7.5 cm
 17. Claystone, same as unit 23..... 1
 16. Limestone..... 5 cm
 15. Claystone, same as unit 23..... 3.6
 14. Limestone..... 0.2
 13. Claystone, same as unit 23..... 3
 12. Limestone..... 0.2
 11. Claystone, same as unit 23, con-
tains foraminifers..... 3.6
 10. Pelletal phosphoritic sandstone,
pebbly..... 7.5 cm
 9. Claystone, very light gray (N8),
massive, friable, siliceous..... 0.6
 8. Claystone, same as unit 9, in part
shaly, contains fish remains..... 0.6
 7. Claystone, same as unit 9..... 3.6
 6. Claystone, same as unit 8, but
lacks fish remains..... 1
 5. Claystone, same as unit 9..... 1.5
 4. Porcelanite, same as unit 25..... 1
 3. Claystone, same as unit 9,
contains crabs..... 3.6
 2. Porcelanite, same as unit 25..... 1.2
 1. Claystone, same as unit 9..... 5.2

Sandholdt Member (beds 1-24)

(Dirt road base, Sandholdt Member possibly continues downward)

Total thickness..... 69.5

Measured Section 191

Thickness (m)

(Hames Member continues upward)

55. Porcelanite, very light gray (N8),
in 3-to 4-cm-thick beds..... 2

Hames Member (bed 55)

54. Claystone, very pale orange (10YR8/2),
massive, friable, calcareous..... 8.5
53. Limestone..... 0.3
52. Claystone, same as unit 54..... 1.8
51. Gypsum and bentonite..... 0.3
50. Claystone, same as unit 54..... 7.3
49. Limestone..... 0.3
48. Claystone, same as unit 54..... 16.1
47. Gypsum and bentonite..... 0.2
46. Claystone, same as unit 54..... 1.8
45. Limestone..... 0.5
44. Claystone, same as unit 54, contains few
volcanic ash interbeds 2.5 cm thick,
calcareous, contains foraminifers..... 2.4
43. Gypsum and bentonite..... 2.5 cm
42. Claystone, same as unit 54, contains
fish scales and foraminifers..... 1
41. Gypsum and bentonite..... 0.2
40. Claystone, same as unit 54..... 1.2
39. Limestone..... 0.2
38. Claystone, same as unit 54, contains
foraminifers..... 1.8
37. Limestone, made up in total by
foraminifera tests..... 0.6
36. Claystone, same as unit 54, contains
foraminifers..... 1
35. Gypsum and bentonite..... 7.5 cm
34. Claystone, same as unit 54, contains
foraminifers..... 3.4
33. Claystone and shale, very pale orange
(10YR8/2), contains less common
occurrences of volcanic ash interbeds
2.5 cm thick..... 0.3
32. Pelletal phosphoritic claystone..... 7.5 cm
31. Claystone and shale, same as unit 33..... 0.6
30. Pelletal phosphoritic, arkosic sand-
stone, pebbly in part..... 7.5 cm
29. Claystone and shale, same as unit 33,
contains gastropods..... 0.2
28. Limestone bleb zone..... 0.3
27. Siltstone, grayish orange (10YR7/4),
laminated, calcareous, phosphatic,
contains fish scales and foraminifers.... 0.6

Measured Section 191 cont'd	Thickness (m)
26. Claystone, same as unit 54, weakly calcareous.....	2
25. Pebbly phosphoritic claystone.....	7.5 cm
24. Limestone.....	0.4
23. Claystone, same as unit 54.....	1.2
22. Pebbly phosphoritic claystone, same as unit 25.....	7.5 cm
21. Claystone, same as unit 54, contains few gypsum interbeds 1 cm thick.....	0.8
20. Claystone, same as unit 54.....	1.2
19. Pebbly phosphoritic claystone zone made up of several beds like unit 25.....	0.3
18. Claystone, very pale orange (10YR/2), in 10-to 15-cm-thick beds, contains 1-to 2-cm-thick shale partings, siliceous.....	0.3
17. Limestone.....	12.5 cm
16. Claystone, same as unit 18.....	0.3
15. Gypsum.....	2.5 cm
14. Claystone, same as unit 18.....	1.8
13. Claystone, grayish orange (10YR7/4), massive, friable, siliceous, contains crabs.....	1.8
12. Pelletal phosphoritic, arkosic sandstone, same as unit 30.....	0.2
11. Limestone bleb zone.....	0.6
10. Sandstone, very pale red (10R6/2), very fine grained, good sorting, laminated, calcareous, grains subangular to subrounded.....	1.5
9. Claystone, same as unit 18.....	1.8
8. Shale, very pale orange (10YR8/2), calcareous, contains foraminifers.....	0.6
7. Gypsum.....	2.5 cm
6. Shale, same as unit 8, possible ripple structures.....	1
5. Sandstone, very pale orange (10YR8/2), fine grained, good sorting, siliceous, grains subangular to subrounded.....	0.2
4. Claystone, same as unit 18.....	0.3
3. Limestone bleb zone.....	0.2
2. Claystone, same as unit 18.....	1
1. Claystone, grayish orange (10YR7/4), massive, friable, calcareous, phosphatic, contains fish scales and foraminifers.....	1.8

Measured Section 191 cont'd	Thickness (m)
Sandholdt Member (beds 1-54)	
(Dirt road base, Sandholdt Member possibly continues downward)	
Total thickness.....	72.5

Measured Section 259

Thickness (m)

(Hames Member continues upward)

9. Porcelanite, very light gray (N8),
in 5-to 6-cm-thick beds..... 3

Hames Member (bed 9)

8. Covered..... 7
7. Claystone, very pale orange (10YR8/2),
in 5-to 6-cm-thick beds..... 1.5
6. Pelletal phosphoritic coquina, large
boulder zone..... 0.2
5. Claystone, very pale orange (10YR8/2),
massive, friable..... 1.5

Sandholdt Member (beds 5-8)

4. Sandstone, yellowish gray (5Y8/1),
fine to very fine grained, good
sorting, massive, friable, weakly
phosphatic, grains subrounded to
subangular..... 3
3. Coquina bed, same as unit 6, bedded,
and lacks pelletal phosphate..... 0.5
2. Sandstone, yellowish gray (5Y7/2),
fine to medium grained, good sorting,
massive, friable, predominantly sub-
angular to subrounded quartz, some
feldspar, very little biotite, weakly
calcareous, very weakly phosphatic..... 31.4

Laureles Sandstone Member (beds 2-4)

1. Granodiorite basement

Total thickness of sedimentary rock..... 48.1

Measured Section 276

Thickness (m)

(Hames Member continues upward)

13.	Porcelanite, light gray (N8), in 5-to 6-cm-thick beds.....	0.6
12.	Leached pelletal phosphoritic sand- stone.....	15 cm
11.	Porcelanite, same as unit 13, contains few pelecypods.....	4
10.	Claystone, very pale orange (10YR8/2), contains few small pelecypods.....	2
9.	Sandstone, same as unit 12, but lacks pelletal phosphate.....	7.5 cm
8.	Porcelanite, same as unit 13.....	1
7.	Pelletal phosphoritic sandstone, same as unit 12.....	7.5 cm
6.	Porcelanite, same as unit 13.....	2.4

Hames Member (beds 6-13)

5.	Limestone.....	0.3
4.	Sandstone, yellowish gray (5YR8/1), fine to very fine grained, good sorting, massive, friable, predominantly sub- angular to subrounded quartz, weakly phosphatic.....	9.1
3.	Large whale bone horizon.....	0.5
2.	Sandstone, yellowish gray (5Y7/2), medium to coarse grained, good sorting, massive, friable, predomi- nantly subangular quartz, some feld- spar, little biotite, weakly cal- careous.....	23.5

Laureles Sandstone Member (beds 2-5)

1. Granodiorite basement

Total thickness of sedimentary rock..... 43.7

Measured Section 332

Thickness (m)

(Hames Member continues upward)

31. Porcelanite, very light gray (N8),
in 5-to 6-cm-thick beds..... 1.5

Hames Member (bed 31)

30. Covered..... 15
 29. Limestone bleb zone..... 0.5
 28. Siltstone, pinkish gray (5YR8/1),
calcareous, carbonaceous, contains
pelecypods, crabs, and foraminifers..... 1
 27. Claystone, pinkish gray (5YR8/1),
massive, siliceous, contains
crabs and burrow structures..... 1.5
 26. Limestone bleb zone..... 0.5
 25. Claystone, same as unit 27..... 1.5
 24. Claystone, very pale orange (10YR8/2),
in 3-to 10-cm-thick beds with 1-to
2-cm-thick shale partings, siliceous..... 1
 23. Pelletal phosphoritic sandstone..... 12.5 cm
 22. Claystone, same as unit 24, contains
pelecypods..... 0.2
 21. Pelletal phosphoritic sandstone,
same as unit 23..... 2.5 cm
 20. Claystone, same as unit 24..... 2.5 cm
 19. Pelletal phosphoritic sandstone
and claystone..... 0.5
 18. Claystone, same as unit 24..... 10
 17. Claystone, same as unit 27, fault..... 2.3
 16. Siltstone and shale, grayish orange
pink (5YR7/2), siliceous, micaceous,
carbonaceous, weakly phosphatic, con-
tains gastropods, crabs, and forami-
nifers..... 1.7
 15. Pelletal phosphoritic sandstone, same
as unit 23..... 0.2
 14. Siltstone and shale, same as unit 16..... 1
 13. Pelletal phosphoritic sandstone,
same as unit 23..... 0.2
 12. Siltstone and shale, same as unit 16..... 1
 11. Limestone bleb zone..... 0.2
 10. Siltstone, very pale orange (10YR8/2),
laminated, possible minute low angle
crossbedding, calcareous, phosphatic,
carbonaceous, contains foraminifers..... 0.3
 9. Claystone, same as unit 27, but lacks
crabs, contains pelecypods, carbona-
ceous..... 1.7

Measured Section 332 cont'd	Thickness (m)
8. Gypsum and bentonite.....	0.2
7. Claystone, same as unit 9.....	1.5
6. Gypsum.....	2.5 cm
5. Claystone, same as unit 9.....	0.5
4. Gypsum.....	2.5 cm
3. Claystone, same as unit 9.....	1.4
2. Siltstone, same as unit 10.....	1.4
1. Claystone, same as unit 9.....	2.5

Sandholdt Member (beds 1-30)

(Asphalt road base, Sandholdt Member possibly continues downward)

Total thickness..... 39.6

Measured Section 399

Thickness (m)

(Hames Member continues upward)

14.	Claystone and porcelanite, light gray (N8), in 5-to 6-cm-thick beds.....	21.3
13.	Pelletal phosphoritic sandstone.....	7 cm
12.	Claystone and porcelanite, same as unit 14.....	7
11.	Pelletal phosphoritic sandstone, same as unit 13.....	7 cm
10.	Claystone and porcelanite, same as unit 14.....	1
9.	Pelletal phosphoritic sandstone, same as unit 13.....	6 cm
8.	Claystone and porcelanite, same as unit 14.....	6 cm

Hames Member (beds 8-14)

7.	Claystone, very pale orange (10YR8/2), in 5-to 6-cm-thick beds, shale partings 0.5-to 1-cm-thick, contains crabs and pelecypods.....	3
6.	Siltstone and shale, grayish orange (10YR7/4), massive, friable, contains foraminifers.....	3
5.	Claystone, dark yellowish orange (10YR6/6), massive, friable, with thin 2-to 3-cm-thick volcanic ash interbeds.....	1.8
4.	Claystone, same as unit 5, but contains several pelletal phosphatic sandstone interbeds same as unit 13.....	1.4
3.	Claystone, same as unit 5.....	2.1
2.	Limestone concretions, contains bones.....	0.5
1.	Claystone, same as unit 5.....	3

Sandholdt Member (beds 1-7)

(Bottom of creek bed, Sandholdt Member possibly continues downward)

Total thickness..... 45.8

<u>Measured Section 467</u>	Thickness (m)
(Top of hill, section incomplete)	
27. Porcelanite, very light gray (N8), in 1-to 2-cm-thick beds.....	0.5
Hames Member (bed 27)	
26. Shale and claystone, very pale orange (10YR8/2), friable.....	2
25. Sandstone, very pale orange (10YR8/2), medium to fine grained, fair sorting, grains angular to subangular, resistant.....	1
24. Sandy shale, very pale orange (10YR8/2), laminated, friable.....	1.8
23. Claystone, very pale orange (10YR8/2), massive, friable.....	3
22. Claystone and siltstone, very pale orange (10YR8/2), friable, contains pelecypods and foraminifers.....	3
Sandholdt Member (beds 22-26)	
21. Sandstone, very pale orange (10YR8/2), fine grained, good sorting, predominantly subangular quartz, some biotite, resistant, very calcareous, slightly phos- phatic, contains small bones.....	0.3
20. Sandstone, grayish orange (10YR7/4), fine grained, fair sorting, predominantly subangular quartz, some feldspar and biotite, friable, calcareous.....	1.8
19. Sandstone, pale olive (10YR6/2), coarse grained, poorly sorted, pre- dominantly subangular quartz, feld- spars, and biotite, friable, calcar- eous, pebbly in part.....	1.5
18. Conglomerate, boulder to cobble to pebble size clasts made up of granite, gneiss, felsite, quartz, quartzite, set in a very coarse grained sandstone matrix made up of angular quartz grains.....	3
17. Sandstone, same as unit 20.....	9.1
16. Sandstone, same as unit 21, con- tains pelecypods.....	0.6
15. Sandstone, same as unit 20.....	3

Measured Section 467 cont'd Thickness (m)

14.	Sandstone, same as unit 21, contains pelecypods, sharks teeth, and bones.....	1
13.	Sandstone, same as unit 20.....	13.7
12.	Sandstone zone of large concretions, light gray (N7), fine grained, fair sorting, predominantly angular quartz, feldspar, and biotite, resistant, calcareous.....	1
11.	Sandstone, same as unit 20.....	9.1
10.	Sandstone, same as unit 12.....	1.2
9.	Sandstone, pale olive (10Y6/2), medium grained, poorly sorted, predominantly subangular quartz, feldspar, biotite, in part pebbly, friable, calcareous.....	1
8.	Sandstone zone, same as unit 12, but contains discontinuous beds rather than concretions.....	1
7.	Sandstone, same as unit 9.....	1.2
6.	Sandstone zone, same as unit 8.....	1
5.	Sandstone, same as unit 9.....	1.2
4.	Sandstone, same as unit 8.....	1

Los Tularcitos Member (beds 4-8)

3.	Sandstone, pale olive (10Y6/2), very coarse grained, poorly sorted, predominantly angular quartz, feldspar, biotite, in part pebbly, friable, upper half weakly calcareous.....	23.7
2.	Conglomerate, boulder to cobble size clasts made up of granite and gneiss, set in a very coarse grained sandy matrix, appears to be graded.....	2.1
1.	Conglomerate, same as unit 2.....	1.5

Robinson Canyon Member (beds 1-3)

(Bottom of creek bed, Robinson Canyon Member possibly continues downward)

Total thickness.....104.5